

# IbNIEL-mediated degradation of IbNAC087 regulates jasmonic acid-dependent salt and drought tolerance in sweet potato<sup>oo</sup>

Xu Li<sup>1,2†</sup>, Zhen Wang<sup>1†</sup>, Sifan Sun<sup>1†</sup>, Zhuoru Dai<sup>1</sup>, Jun Zhang<sup>1,2</sup>, Wenbin Wang<sup>1</sup>, Kui Peng<sup>1</sup>, Wenhao Geng<sup>1,2</sup>, Shuanghong Xia<sup>1</sup>, Qingchang Liu<sup>1</sup>, Hong Zhai<sup>1</sup>, Shaopei Gao<sup>1</sup>, Ning Zhao<sup>1</sup>, Feng Tian<sup>3</sup>, Huan Zhang<sup>1,2\*</sup> and Shaozhen He<sup>1,2\*</sup>

1. Key Laboratory of Sweet Potato Biology and Biotechnology, Ministry of Agriculture and Rural Affairs/Beijing Key Laboratory of Crop Genetic Improvement/Laboratory of Crop Heterosis & Utilization and Joint Laboratory for International Cooperation in Crop Molecular Breeding, Ministry of Education, College of Agronomy & Biotechnology, China Agricultural University, Beijing 100193, China

2. Sanya Institute of China Agricultural University, Sanya 572025, China

3. State Key Laboratory of Plant Physiology and Biochemistry, National Maize Improvement Center, Key Laboratory of Biology and Genetic Improvement of Maize, Beijing Key Laboratory of Crop Genetic Improvement, China Agricultural University, Beijing 100193, China

<sup>†</sup>These authors contributed equally to this work.

\*Correspondences: Huan Zhang ([zhanghuan1111@cau.edu.cn](mailto:zhanghuan1111@cau.edu.cn)); Shaozhen He ([sunnynba@cau.edu.cn](mailto:sunnynba@cau.edu.cn), Prof. He is fully responsible for the distribution of all materials associated with this article)



Xu Li



Shaozhen He

scavenging, whereas silencing this gene resulted in opposite phenotypes. JA-rich *IbNAC087*-OE (overexpression) plants exhibited more stomatal closure than wild-type (WT) and *IbNAC087*-Ri plants under NaCl, polyethylene glycol, and methyl jasmonate treatments. *IbNAC087* functions as a nuclear transcriptional activator and directly activates the expression of the key JA biosynthesis-related genes *lipoxygenase (IbLOX)* and *allene oxide synthase (IbAOS)*. Moreover, *IbNAC087* physically interacted with a RING-type E3 ubiquitin ligase NAC087-INTERACTING E3 LIGASE (*IbNIEL*), negatively regulating salt and drought tolerance in sweet potato. *IbNIEL* ubiquitinated *IbNAC087* to promote 26S proteasome degradation, which weakened its activation on *IbLOX* and *IbAOS*. The findings provide insights into the mechanism underlying the *IbNIEL*-*IbNAC087* module regulation of JA-dependent salt and drought response in sweet potato and provide candidate genes for improving abiotic stress tolerance in crops.

Keywords: abiotic tolerance, *IbNAC087*, *IbNIEL*, JA, sweet potato

Li, X., Wang, Z., Sun, S., Dai, Z., Zhang, J., Wang, W., Peng, K., Geng, W., Xia, S., Liu, Q., Zhai, H., Gao, S., Zhao, N., Tian, F., Zhang, H., and He, S. (2024). *IbNIEL*-mediated degradation of *IbNAC087* regulates jasmonic acid-dependent salt and drought tolerance in sweet potato. *J. Integr. Plant Biol.* **00**: 1–20.

## ABSTRACT

Sweet potato (*Ipomoea batatas* [L.] Lam.) is a crucial staple and bioenergy crop. Its abiotic stress tolerance holds significant importance in fully utilizing marginal lands. Transcriptional processes regulate abiotic stress responses, yet the molecular regulatory mechanisms in sweet potato remain unclear. In this study, a NAC (NAM, ATAF1/2, and CUC2) transcription factor, *IbNAC087*, was identified, which is commonly upregulated in salt- and drought-tolerant germplasms. Overexpression of *IbNAC087* increased salt and drought tolerance by increasing jasmonic acid (JA) accumulation and activating reactive oxygen species (ROS)

## INTRODUCTION

Salinity and drought pose significant threats to global food security, causing severe losses in agricultural production (Bartels and Sunkar, 2005). Salt-affected soils cover approximately 1.029 billion ha worldwide, of which 40% are saline, and 60% are sodic (Squires and Glenn, 2004). Sweet potato (*Ipomoea batatas* [L.] Lam. ( $2n = 6x = 90$ )) is a crucial crop for food, bioenergy, and healthcare (Gao et al., 2023). It is primarily grown on marginal lands and ranks eighth in global food production (FAO, 2022). Developing and cultivating stress-tolerant sweet potato varieties play important roles in fully utilizing marginal land and securing the food supply (Schmidt et al., 2023). Therefore, in-depth studies on the molecular mechanisms underlying abiotic stress tolerance are important for genetically engineering stress-tolerant sweet potato (Zhang et al., 2019).

Jasmonic acid (JA) was initially identified as a plant stress-related hormone (Wasternack and Song, 2017). Accumulating evidence indicates that JA plays a pivotal role in enabling plants to adapt to abiotic stresses by activating antioxidant systems (Kazan and Manners, 2013; Qiu et al., 2014; Yan et al., 2015), regulating stomatal closure (Munemasa et al., 2007; Rohwer and Erwin, 2008; Xing et al., 2020), and increasing osmotic pressure (Ahmadi et al., 2018; Ming et al., 2021). JA-related genes are also involved in abiotic stress tolerance (Seo et al., 2011; Wang et al., 2019; Singh et al., 2021). OsbHLH062 interacts with OsJAZ9 in rice to improve salt tolerance by regulating ion homeostasis under salt stress (Wu et al., 2015). In *Arabidopsis*, glucosinolate transporter1 (GTR1/NPF2.10), a JA-Ilc transporter, mediates JA signaling and represses *HKT1* expression to regulate lateral root development under salt stress (Kuo et al., 2020). In oriental melon seedlings, CmLOX10 increases drought tolerance by inducing JA-mediated stomatal closure (Xing et al., 2020). Under salt stress, the JA level in the salt-tolerant sweet potato line ND98 was increased, leading to stomatal closure and ion homeostasis maintenance (Zhang et al., 2017b). However, the intrinsic regulatory mechanisms of JA-mediated abiotic stress tolerance in sweet potato remain unclear.

The NAC (NAM, ATAF1/2, and CUC2) transcription factor (TF) family is one of the largest families of plant-specific TFs. It is characterized by a conserved NAC domain at the N-terminus and a diverse transcriptional regulatory region at the C-terminus (Olsen et al., 2005). NACs have important roles in a variety of developmental processes (Mao et al., 2017; Fang et al., 2020; Mao et al., 2020) and biotic (Li et al., 2021; Meng et al., 2022; Bi et al., 2023) and abiotic stress responses (Hu et al., 2006; Zheng et al., 2009; Nakashima et al., 2012; Xiang et al., 2021a, 2021b). Overexpressing sweet potato *IbNAC7* in *Arabidopsis* increases salt tolerance by activating reactive oxygen species (ROS) scavenging and affecting the transcription of stress-related genes (Meng et al., 2020). *IbNAC3* participates in abscisic acid (ABA)-dependent salt and drought responses (Meng et al., 2023). However, the biological

functions and regulatory mechanisms of NACs in the abiotic stress responses of sweet potato remain largely unknown.

Ubiquitination is an important post-translational modification involved in cellular processes that regulate protein stability and biological activity (Yu et al., 2016). It requires the sequential action of three types of enzymes: ubiquitin-activating enzymes (E1), ubiquitin-conjugating enzymes (E2), and ubiquitin ligases (E3) (Vierstra, 2009). The main specificity determinants for ubiquitination are E3 ligases, classified into three major types: RING, HECT, and RBR E3s (Trujillo and Shirasu, 2010; Morreale and Waldenand, 2016). Most ubiquitination-modified proteins are subsequently degraded by the 26S proteasome, a major protein degradation pathway (Stone, 2014). In plants, ubiquitination engages in different abiotic stress-response pathways. OsMSRFP (RING E3) in rice ubiquitinates and degrades OsMYBc, inhibiting OsHKT1;1 expression and weakening salt stress tolerance (Xiao et al., 2022). MYB30-INTERACTING E3 LIGASE 1 (MIEL1, RING E3) in apples mediates the ubiquitination and degradation of MdBBX7 by the 26S proteasome pathway and negatively regulates drought stress response (Chen et al., 2021). A U-box-type E3 ubiquitin ligase, MdPUB23, regulates the cold-stress response by controlling the stability of the positive regulator MdICE1 (Wang et al., 2022). Nevertheless, the functions, substrates, and regulatory mechanisms of E3s in sweet potato remain unclear.

In this study, a NAC TF, *IbNAC087*, was identified, which is commonly upregulated in multiple salt- and drought-tolerant germplasms. Overexpression of *IbNAC087* in sweet potato increased salt and drought tolerance by promoting JA-mediated ROS scavenging and stomatal closure. *IbNAC087* directly targeted the key JA biosynthesis-related genes *IbLOX* and *IbAOS* to activate their expression. Moreover, the E3 ubiquitin ligase NAC087-INTERACTING E3 LIGASE (*IbNIEL*), which negatively regulated salt and drought tolerance, ubiquitinated and promoted its degradation, and inhibited its activation on *IbLOX* and *IbAOS*. Collectively, our data demonstrate that the *IbNIEL-IbNAC087* module regulates JA-dependent salt and drought response in sweet potato.

## RESULTS

### *IbNAC087* is commonly upregulated in multiple salt- and drought-tolerant germplasms

To identify potential regulatory factors of abiotic stress responses, the transcriptomes of the salt-tolerant sweet potato germplasms JA-rich ND98 (Zhang et al., 2017a) and Xushu22 (X22) (Yu et al., 2016), as well as that of the drought-tolerant sweet potato diploid relative *Ipomoea triloba* NCNSP0323 ( $2n = 2x = 30$ ; Yang et al., 2018), were re-analyzed. The expression of 148 genes was commonly upregulated (Figure 1A) in the salt- and drought-tolerant germplasms, including that of the functionally validated

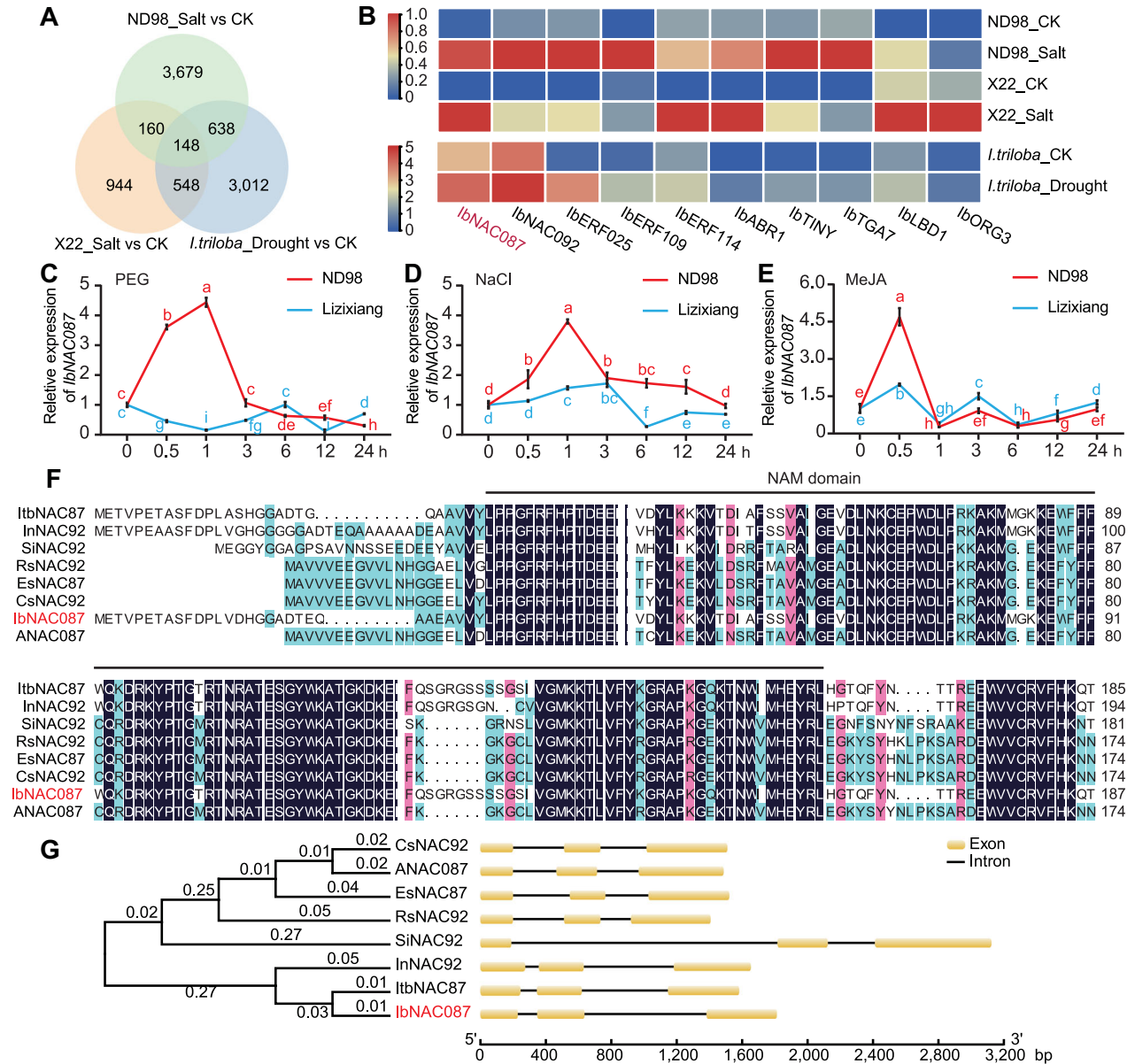


**Figure 1. *IbNAC087* is commonly upregulated in multiple salt- and drought-tolerant germplasms**

(A) Venn diagrams showing the numbers of candidate abiotic-related genes detected in salt- and drought-tolerant germplasms. ND98, salt-tolerant line; X22, salt-tolerant variety; *Ipomoea triloba*, drought-tolerant diploid relative. (B) The expression patterns of the candidate abiotic-related transcription factors (TFs) as determined by RNA sequencing (RNA-seq). (C–E) Expression analysis of *IbNAC087* in salt-tolerant line ND98 and salt-susceptible variety Lizixiang in response to 200 mmol/L NaCl, 20% polyethylene glycol (PEG)6000 and 100 μmol/L methyl jasmonate (MeJA). The sweet potato *β-Actin* gene was used as an internal control. Data are presented as the means ± SD (n = 3). Different lowercase letters indicate significant differences (one-way analysis of variance followed by *post-hoc* Tukey test; P < 0.05). (F) Multiple sequence alignment of the NAC087 protein in sweet potato and other plants. The NAM domain is represented with lines. (G) Phylogenetic analysis and genomic structures of NACs (NAM, ATAF1/2, and CUC2) in sweet potato and other plants. The *IbNAC087* cloned in this study is marked in red. Distances were estimated using a neighbor-joining algorithm. Exons are represented by yellow boxes, and introns are represented by black lines.

stress-tolerant genes *POD* (Michiels et al., 1994) and *HPPD* (Kim et al., 2021) in sweet potato. There were 10 TFs among these genes (Table S1). Notably, *IbNAC087* was upregulated in the salt- and drought-tolerant germplasms under salt and drought stresses, respectively (Figure 1B). Real-time quantitative polymerase chain reaction (RT-qPCR) analysis was used to determine the relative transcript abundance of *IbNAC087* under NaCl, polyethylene glycol (PEG), and methyl jasmonate

(MeJA) treatments in salt-tolerant line ND98 and salt-susceptible variety Lizixiang. The expression levels of *IbNAC087* increased significantly under PEG (4.44 ± 0.15 fold) and NaCl (3.80 ± 0.07 fold) treatments at 1 h and under MeJA treatment (4.70 ± 0.35 fold) at 0.5 h (Figure 1C–E) in ND98 leaves. In contrast, its expression in Lizixiang had no significant change. Therefore, the study focused on *IbNAC087* for its potential role in the abiotic stress response in sweet potato.

The *IbNAC087* from the JA-rich salt-tolerant line ND98 was cloned. It encoded a 318-amino acid NAC TF with an open reading frame (ORF) sequence of 957 bp, a predicted molecular weight (MW) of 35.575 kDa, and an isoelectric point (pI) of 5.04. The protein contained a highly conserved nucleic acid memory (NAM) DNA-binding domain (Figure 1F). *IbNAC087* in sweet potato shared the highest homology with *IbNAC087* in other plants (Figure 1G) and *ANAC087* among *Arabidopsis* (Figure S1). Moreover, its homologs cluster separately in monocots and dicots, and *IbNAC087* has a high homology with its homologs in dicots (Figure S2). Multiple sequence alignment showed that the A and D subdomains of the NAC087 homologs showed high conservation. At the same time, differentiation was observed in the B, C, and E subdomains between monocots and dicots, especially in E (Figure S3). The C-terminus of the NAC087 homologs displayed significant diversity in both monocots and dicots (Figure S3). The 1,832-bp genomic sequence of *IbNAC087* contained two introns and three exons, similar to homologous NACs in other plants, such as *ANAC087*, *CsNAC92*, *EsNAC87*, and *RsNAC92* (Figure 1G). The results indicated that *IbNAC087* might be involved in salt and drought responses in sweet potato.

### ***IbNAC087* is highly expressed in leaves, and MeJA induces its promoter**

To investigate the potential role of *IbNAC087*, RT-qPCR analysis was performed to determine its relative transcript levels in different tissues of ND98. The highest expression levels of *IbNAC087* (almost 3.42-fold vs. storage root as the control) were in the leaves of field-grown plants (Figure 2A).

Various abiotic stress-responsive and development-related elements were found in the 1,590-bp promoter region of *IbNAC087*, such as drought-responsive MYB binding site (MBS; Karkute et al., 2018), MeJA-responsive elements (CGTCA and TGACG motifs; Rouster et al., 1997; Wang et al., 2010), and ABA-responsive elements (ABREs; Michel et al., 1993; Busk and Pages, 1997), and auxin-responsive elements (AuxRE motif; Ballas et al., 1993) (Figure S4). The spatial expression pattern of *IbNAC087* in *IbNAC087pro-gusA* transgenic sweet potato plants was also determined. In transgenic plants, *gusA* was expressed in leaves, stems and roots, but especially in the leaves (Figure 2B). The expression of *gusA* increased significantly with NaCl, PEG, and MeJA treatments (Figure 2C). The expression patterns were consistent with the tissue-specific and abiotic stress-induced expression of *IbNAC087* (Figure 1C–E). *IbNAC087* was highly expressed in sweet potato leaves, with expression increasing under NaCl and PEG, particularly MeJA treatments.

### ***IbNAC087* is a nucleus-localized transactivator**

To determine the subcellular location of *IbNAC087*, the *IbNAC087*-GFP (green fluorescent protein) fusion protein was transiently expressed in protoplasts. Under confocal microscopy, *IbNAC087*-GFP was observed in the nucleus (Figure 2D).

Transactivation activity in yeast cells was evaluated with the full-length *IbNAC087* and three of its fragments (*IbNAC087*<sup>N32</sup>, 1–32 amino acid residues at the N-terminal; *IbNAC087*<sup>N234</sup>, 1–234 amino acid residues at the N-terminal; *IbNAC087*<sup>C84</sup>, 235–318 amino acid residues at the C-terminal). *IbNAC087*, with a total length of 318 amino acid residues, showed transcriptional activation, and *IbNAC087*<sup>C84</sup> was required for transcriptional activation (Figure 2E). *IbNAC087* was further fused to the DNA-binding domain of GAL4 and transiently transfected in protoplasts. The full-length *IbNAC087* and *IbNAC087*<sup>C84</sup> fragments possessed much stronger transactivation activity than *IbNAC087*<sup>N234</sup>. The result of amino acid species statistics showed *IbNAC087*<sup>C84</sup> enriched in simple amino acids (serine-S, threonine-T, proline-P; 23/84) and acidic residues (glutamic acid-E, aspartic acid-D; 11/84) (Table S2). Thus, the C-terminus of *IbNAC087* was critical for its transactivation activity, and *IbNAC087* was a nucleus-localized transactivator (Figure 2F).

### **Overexpression of *IbNAC087* increases JA-dependent salt and drought tolerance**

To verify whether *IbNAC087* contributed to abiotic stress tolerance, 25 overexpression (OE) lines (OE-N1 to OE-N25) and three RNA interference (RNAi) lines (Ri-N1 to Ri-N3) were generated from 682 and 273 cell aggregates, respectively, of the salt-susceptible variety Lizixiang via *Agrobacterium*-mediated transformation (Figure S5). *In vitro*-grown *IbNAC087*-OE lines exhibited increased growth and rooting under 200 mmol/L NaCl or 20% PEG6000 treatments compared with wild-type (WT) plants (Figure S6A, C–F; Table S3). The increases were associated with decreases in malondialdehyde (MDA) and H<sub>2</sub>O<sub>2</sub> contents and increases in superoxide dismutase (SOD) and catalase (CAT) activities (Figure S6B, G–J; Table S3).

The survival rate of all transgenic and WT plants after transfer to the field was 100%. Three *IbNAC087*-OE lines (OE-N3, N4, N19) and two *IbNAC087*-Ri lines (Ri-N1, N3) were selected for further phenotyping. They were grown in transplanting boxes and subjected to 200 mmol/L NaCl and drought stresses. After 64 d of NaCl and 53 d of drought treatments, the *IbNAC087*-OE lines displayed traits indicating salt and drought insensitivity, whereas the *IbNAC087*-Ri lines showed early browning (Figure 3A). In the *IbNAC087*-OE lines, rooting abilities improved and fresh weight (FW) and dry weight (DW) increased, whereas the opposite phenotypes were observed in the *IbNAC087*-Ri lines (Figures 3B, C, S7; Table S4).

Endogenous JA levels in normal and stress-treated plants were then quantified. JA was much more abundant in *IbNAC087*-OE plants but significantly less abundant in *IbNAC087*-Ri lines under normal, salt, and drought conditions than in WT plants (Figure 3D; Table S4). Because JA is a crucial regulator in activating antioxidant enzymes to promote reactive oxygen species (ROS) scavenging mechanisms under abiotic stress in plants (Ma et al., 2021; Liu et al., 2023), several related physiological indices were measured.

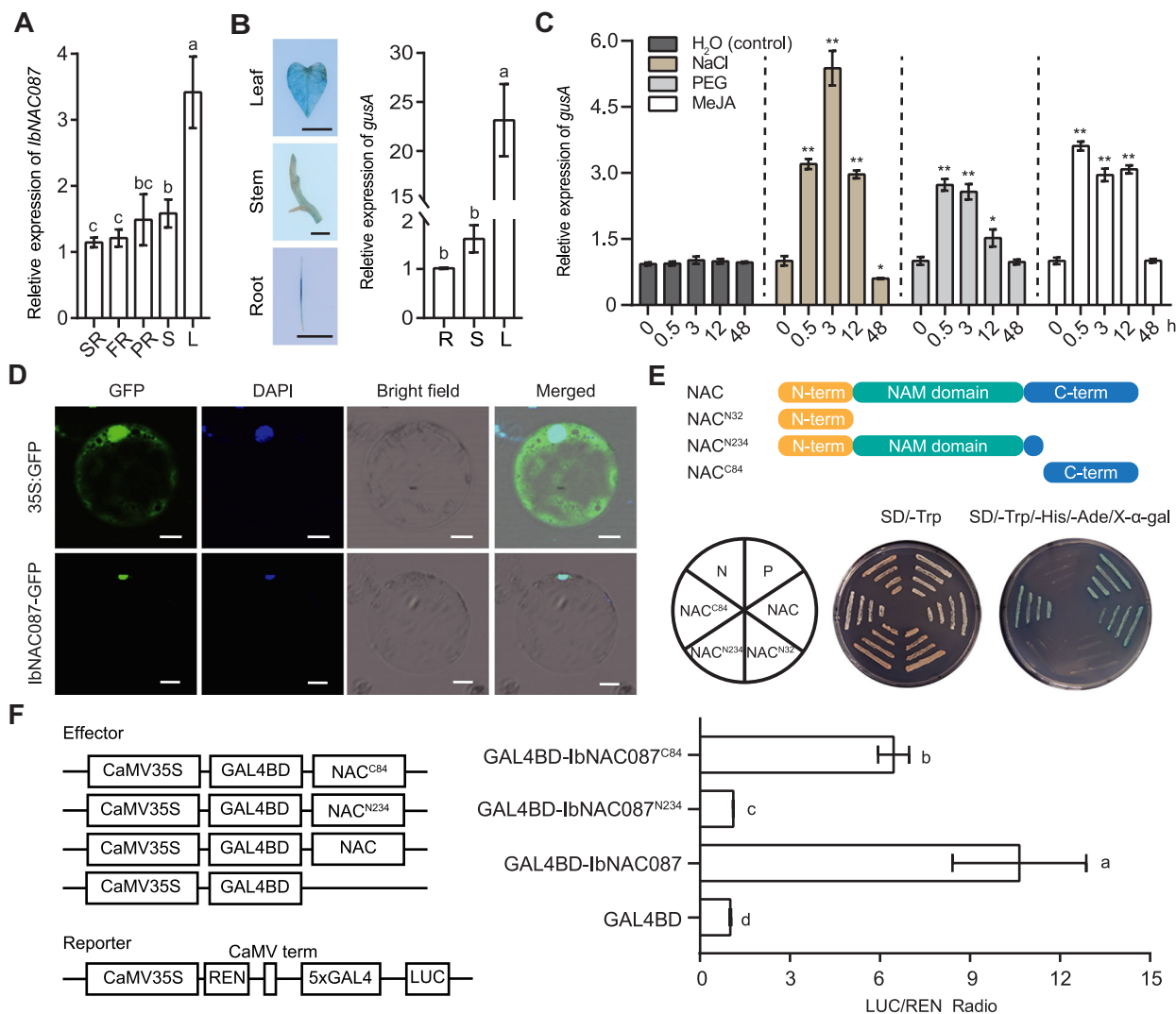


**Figure 2.** *IbNAC087* is a nucleus-localized transactivator

(A) Transcript levels of *IbNAC087* in different tissues of ND98. L, leaf; S, stem; FR, fibrous root; PR, pencil root; SR, storage root. (B) The expression of *gusA* driven by the *IbNAC087* promoter in different tissues of transgenic sweet potato plants. Bars = 0.5 cm. (C) The expression of *gusA* driven by the *IbNAC087* promoter in leaves of transgenic sweet potato plants treated with 200 mmol/L NaCl, or 20% polyethylene glycol (PEG)6000, or 100  $\mu$ mol/L methyl jasmonate (MeJA) for different times. (D) The *IbNAC087*-GFP (green fluorescent protein) fusion protein was transiently expressed into rice protoplasts and visualized by fluorescence microscopy. Bars = 10  $\mu$ m. (E) Transcriptional activation assay of *IbNAC087*. Fusion proteins of the GAL4 DNA-binding domain and different portions of *IbNAC087* were expressed in yeast strain Y2H (yeast two-hybrid). The pGBKT7 empty vector was used as a negative control (N), while pGBKT7-53 was used as a positive control (P). The positive transformants were cultured on synthetic defined (SD)/-Trp/-His/-Ade/X- $\alpha$ -gal medium. NAC, full-length *IbNAC087*; NAC<sup>N32</sup>, 1-32 amino acid residues at the N-terminal; NAC<sup>N234</sup>, 1-234 amino acid residues at the N-terminal; NAC<sup>C84</sup>, 235-318 amino acid residues at the C-terminal. (F) Transactivation analysis of *IbNAC087* in protoplasts. The transactivation ability of *IbNAC087* was demonstrated by the ratio of luciferase (LUC) to renilla luciferase (REN). The LUC/REN ratio of the empty GAL4BD vector (negative control) was used as a calibrator (set as 1). Data are presented as the means  $\pm$  SD ( $n = 3$ ). \* and \*\* indicate a significantly difference compared with the wild-type (WT) at  $P < 0.05$  and  $P < 0.01$  based on Student's *t*-test, respectively. Different lowercase letters indicate significant differences ( $P < 0.05$ ; one-way analysis of variance).

Compared with WT plants, *IbNAC087*-OE lines had higher SOD, CAT, and peroxidase (POD) activities and accumulated less MDA and H<sub>2</sub>O<sub>2</sub> under salt and drought stresses, whereas the opposite patterns were observed in *IbNAC087*-Ri plants (Figure 3E-I; Table S4).

The expression levels of abiotic stress-responsive genes were also analyzed after salt and drought stresses. Expression levels of the ROS scavenging-related genes *IbSOD*

(Duroux and Welinder, 2003), *IbCAT* (Wang et al., 2016), *IbPOD*, and *IbAPX* (Zhai et al., 2016) were significantly higher in the *IbNAC087*-OE lines than in the WT and *IbNAC087*-Ri plants under salt and drought stresses (Figure S9A-D).

JA signaling leads to stomatal closure as an essential response to environmental challenges (Pospíšilová, 2003). Stoma aperture changes were observed in the leaves of WT and *IbNAC087* transgenic plants after exposing the leaves to

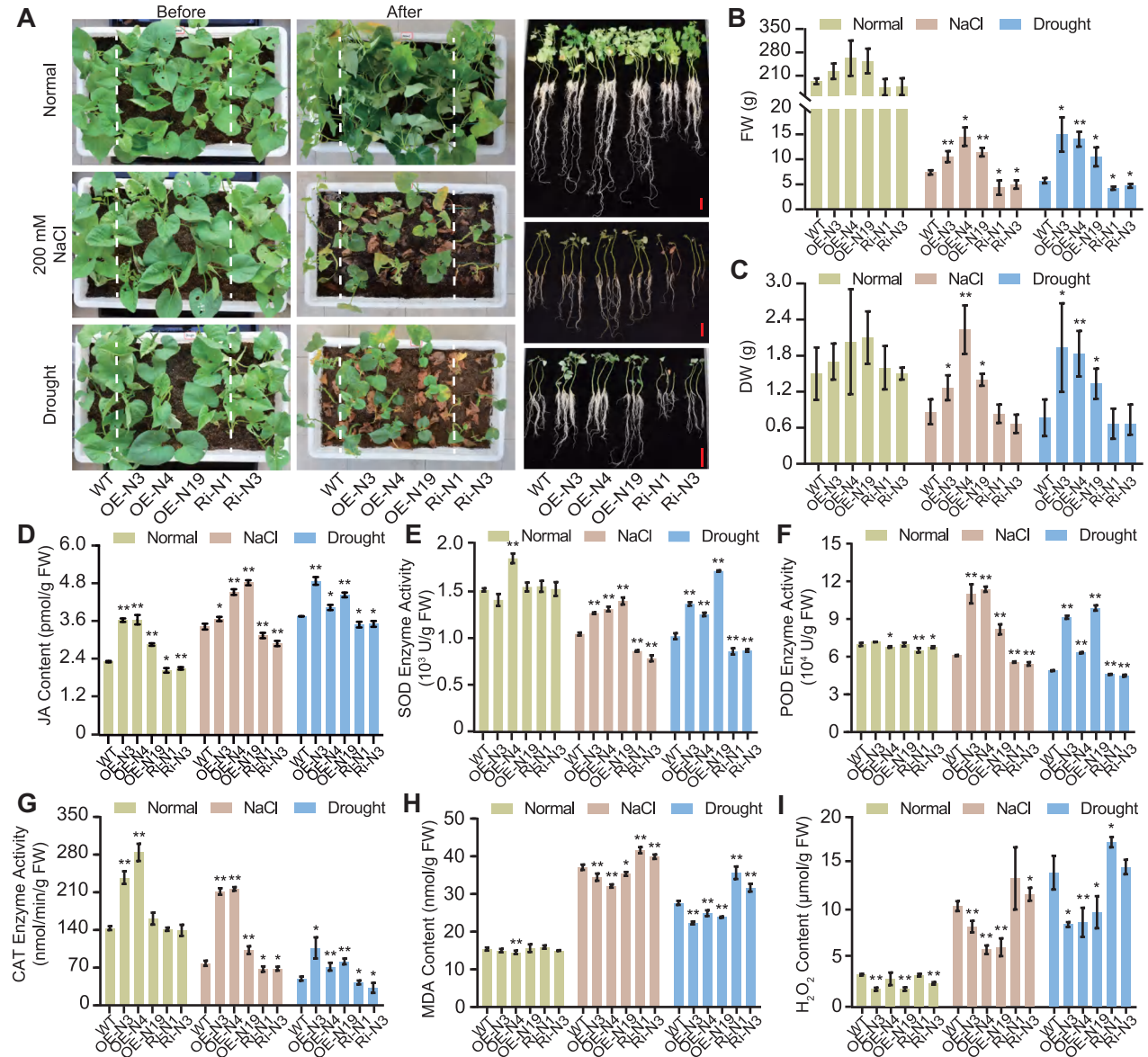


**Figure 3. Overexpression of *IbNAC087* enhances jasmonic acid (JA)-dependent salt and drought tolerance in sweet potato**

(A) Growth condition, (B) fresh weight (FW), (C) fry weight (DW) of *IbNAC087*-transgenic lines and wild-type (WT) grown in transplanting boxes without stress or with 200 mmol/L NaCl and drought stress. Bars = 10 cm. Time-course phenotypes of *IbNAC087*-transgenic and WT plants grown in transplanting boxes under abiotic stresses are shown in Figure S8. (D) JA content, (E) superoxide dismutase activity, (F) peroxidase activity, (G) catalase activity, (H) malondialdehyde content, and (I) H<sub>2</sub>O<sub>2</sub> content in leaves of *IbNAC087*-transgenic plants and the WT under normal conditions or NaCl or drought stresses. Data are presented as the means ± SD (n = 3). \* and \*\* indicate a significant difference compared with the WT at P < 0.05 and P < 0.01, respectively, based on Student's *t*-test.

200 mmol/L NaCl, 20% PEG6000 for 1 h, or 50 μmol/L MeJA for 2 h. Under normal conditions, most stomas in the WT and transgenic lines were partially open; however, under NaCl, PEG, and MeJA treatments, stomatal closure was faster in *IbNAC087*-OE lines than in WT plants, whereas closure was slower in *IbNAC087*-Ri lines (Figure S10A, B). Moreover, under NaCl and PEG treatments, applying exogenous MeJA effectively promoted stomatal closure and enhanced ROS scavenging, reducing MDA and H<sub>2</sub>O<sub>2</sub> contents (Figure S10C, D; Table S5). The results indicated that OE of *IbNAC087*

increased salt and drought tolerance by promoting JA-mediated ROS scavenging and stomatal closure in sweet potato.

### ***IbNAC087* promotes JA biosynthesis by activating the expression of *IbLOX* and *IbAOS***

The effect of *IbNAC087* on JA accumulation was investigated by analyzing the expression of JA biosynthesis-related genes. *IbLOX* and *IbAOS* expression levels were significantly higher in *IbNAC087*-OE lines but lower in *IbNAC087*-Ri lines compared

with WT plants (Figure 4A, B). Previous studies have documented that the NACs bind to the NACBS (including the recognition site (NACRS, CGT(G/A)) and the DNA-binding core sequence (CACG)) or motifs that contain the CGTC sequence in the promoters of their target genes (Simpson et al., 2003; Ernst et al., 2004). *IbLOX* and *IbAOS* promoter elements analysis revealed NAC-binding motifs (Figure 4C; Table S6). Yeast one-hybrid (Y1H) and chromatin immunoprecipitation-quantitative PCR (ChIP-qPCR) assays indicated that IbNAC087 directly bound to gene promoters, both in yeast cells and *in vivo* (Figure 4D, E). To further determine the binding of IbNAC087 on the promoter of *IbLOX* and *IbAOS*, we purified His-IbNAC087 fusion protein *in vitro* (Figure S11), and electrophoretic mobility shift assays (EMSA) were performed (Figure 4F, G). The IbNAC087 bound directly to the WT probe, whereas there was no bound probe when the CGTG in *IbLOXpro* was mutated to AAAA (Figure 4F) and CGTC in *IbAOSpro* was mutated to TTTT (Figure 4G). Transient dual-luciferase assays with the LUC reporter gene driven by the *IbLOX* and *IbAOS* promoters were performed to investigate how IbNAC087 regulated the transcription of *IbLOX* and *IbAOS*. IbNAC087 strongly activated *IbLOXpro-LUC* and *IbAOSpro-LUC* expression in protoplasts (Figure 4H).

We generated their overexpression lines using the Cut-Dip-Budding (CDB) delivery system to investigate the potential biological function of *IbLOX* and *IbAOS* in sweet potato (Cao et al., 2022). Under NaCl and drought treatments, *IbLOX*-OE and *IbAOS*-OE plants exhibited better growth, longer roots, higher CAT and POD activities, and lower MDA and H<sub>2</sub>O<sub>2</sub> contents than WT plants (Figure S12; Table S7). These results indicate that *IbLOX* and *IbAOS* function as positive regulators against salt and drought stresses in sweet potato. Together, the results suggested that IbNAC087 promotes JA-dependent salt and drought tolerance via direct binding to the promoters of the key JA biosynthesis-related genes *IbLOX* and *IbAOS* and activation of their expression.

### IbNAC087 physically interacts with a RING-finger E3 ubiquitin ligase IbNIEL

A yeast two-hybrid (Y2H) system was used to identify proteins interacting with IbNAC087 to better understand the regulatory mechanisms of IbNAC087-mediated abiotic stress responses. A Y2H library was generated using RNA from sweet potato leaves, and the IbNAC087<sup>N234</sup> fragment was used as the bait in Y2H screens. A RING-finger E3 ubiquitin ligase, which interacted with IbNAC087<sup>N234</sup> in yeast, was identified and named NAC087-INTERACTING E3 LIGASE (IbNIEL) (Figure 5A; Table S8). To corroborate that IbNIEL was one of the interacting partners of IbNAC087, bimolecular fluorescence complementation (BiFC) assays were performed in *Nicotiana benthamiana* leaves. When IbNAC087-nYFP (yellow fluorescent protein) and IbNIEL-cYFP were co-expressed, strong YFP fluorescence was detected in the nucleus of transformed cells (Figure 5B). In addition, a co-immunoprecipitation (Co-IP) assay was conducted in *N. benthamiana* leaves co-transformed with

hemagglutinin (HA)-tagged IbNAC087 and MYC-tagged IbNIEL. Proteins were immunoprecipitated using anti-HA beads and detected with MYC antibody. The Co-IP results confirmed the interaction between IbNAC087 and IbNIEL *in vivo* (Figure 5C).

The RING-finger E3 ubiquitin ligase IbNIEL contained a zf\_CHy motif, a RING\_Ubox superfamily motif, and a zinc\_ribbon\_6 motif (Figure S13A, B). Notably, its protein sequence was the same as that of IbtNIEL in the sweet potato diploid relative *Ipomoea trifida* (Figure S13C). IbNIEL-GFP was observed in the nucleus, cytoplasm, and on membranes (Figure S13D). The expression levels of *IbNIEL* decreased significantly under salt, drought, and MeJA treatments (Figure S13E). An E3 ubiquitin ligase activity assay showed that the recombinant IbNIEL protein had autoubiquitination activity with E1 and E2 (Figure 5D). The results indicated that IbNAC087 physically interacted with the conserved RING-finger E3 ubiquitin ligase IbNIEL in sweet potato.

### IbNIEL ubiquitinates IbNAC087 and accelerates its degradation via the 26S proteasome

The 26S proteasome degrades most ubiquitylated proteins, with the concomitant release of ubiquitin moieties for reuse (Vierstra, 2009). We purified the glutathione S-transferase (GST)-IbNIEL fusion protein *in vitro* (Figure S14) and performed an *in vitro* ubiquitination assay. The addition of maltose-binding protein (MBP)-IbNAC087 into the reaction led to the production of MBP-IbNAC087-Ub ladders, a key characteristic of ubiquitination reaction, but reactions missing any of these components failed to ubiquitinate IbNAC087. The results showed that IbNIEL ubiquitinates IbNAC087 *in vitro* (Figure 5E).

Whether IbNIEL could promote IbNAC087 degradation was then determined by cell-free degradation assays using proteins extracted from WT and *IbNIEL*-OE plants. The His-IbNAC087 protein levels decreased in the *IbNIEL*-OE plants compared with the WT plants, indicating that IbNAC087 was unstable and prone to degradation. Thus, IbNIEL promoted the degradation of IbNAC087 (Figure 5F, G). To investigate whether IbNAC087 degraded through the 26S proteasome, the stability of IbNAC087 in the presence of the proteasomal inhibitor MG132 was also measured. IbNAC087 was less abundant in *IbNIEL*-OE plants than in WT plants, and adding MG132 increased the stability of IbNAC087 (Figure 5H). Whether IbNAC087 underwent IbNIEL-mediated 26S proteasomal degradation was also investigated by dual-luciferase reporter assays. *IbLOXpro-LUC*, *IbAOSpro-LUC*, *IbNAC087*, and *IbNIEL* were transiently expressed in protoplasts and then treated with MG132. IbNIEL weakened the activation of *IbLOX* and *IbAOS* by IbNAC087, whereas the addition of MG132 attenuated the effect (Figure 5I). The results indicated that IbNIEL ubiquitinates IbNAC087 and accelerates its degradation via the 26S proteasome in sweet potato.

### IbNIEL negatively regulates salt and drought tolerance of sweet potato

The biological functions of E3 ubiquitin ligases in sweet potato remain unknown. Four *IbNIEL*-OE lines (OE-E1 to OE-E4)

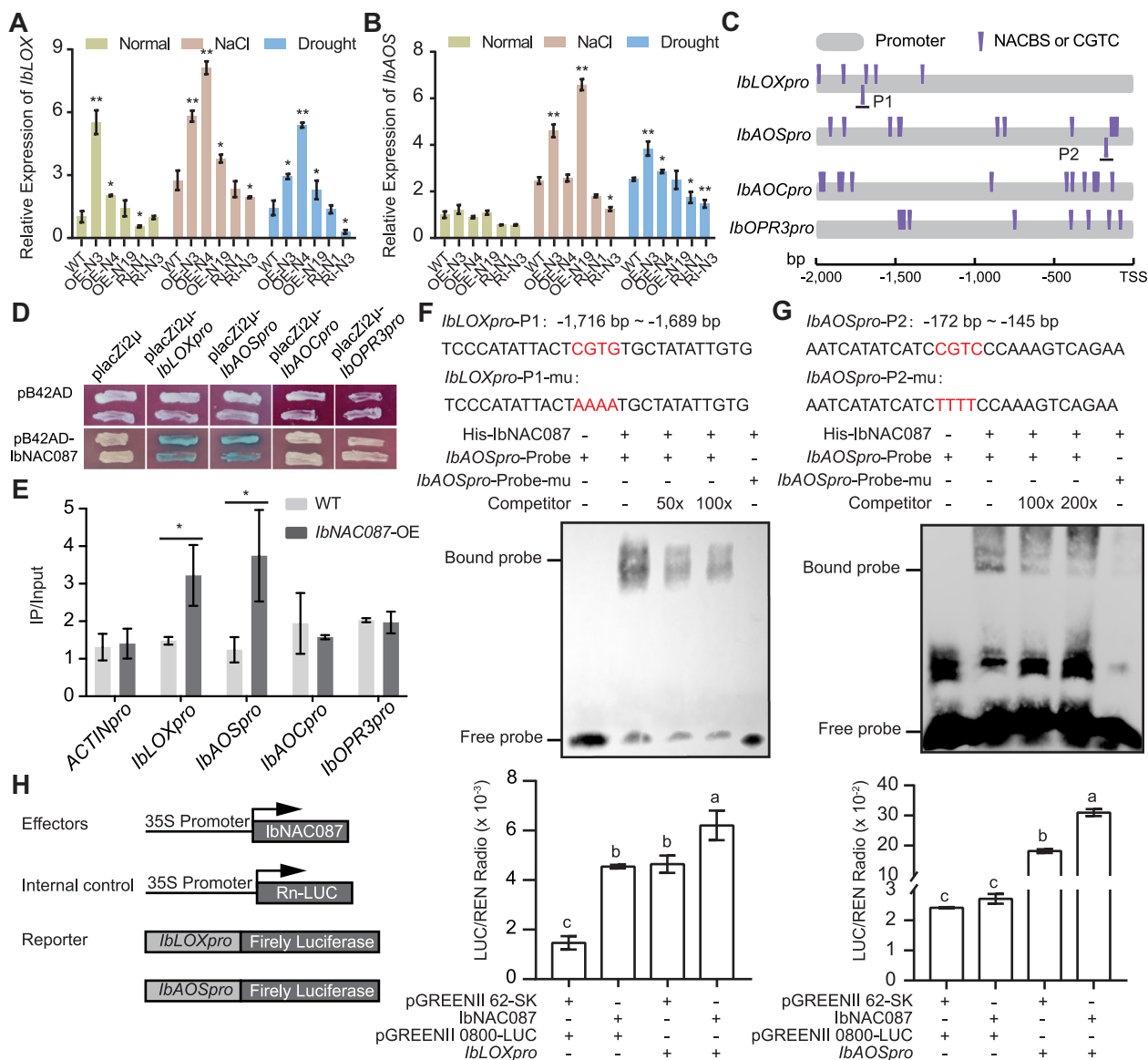


**Figure 4. IbNAC087 directly activates the expression of IbLOX and IbAOS**

(A, B) The expression of jasmonic acid (JA) biosynthesis-related genes *IbLOX* and *IbAOS* in *IbNAC087* transgenic and wild-type (WT) plants under salt and drought stresses. (C) Distribution of NAC (NAM, ATAF1/2, and CUC2)-binding motifs on the promoters of JA biosynthesis-related genes. NACBS, the NAC recognition site (NACRS, CGT(G/A)), and the DNA-binding core sequence (CACG). (D) Yeast-one-hybrid (Y1H) assays showing that *IbNAC087* bound to the *IbLOX* and *IbAOS* promoters. (E) Chromatin immunoprecipitation – quantitative polymerase chain reaction (ChIP-qPCR) assays using *IbNAC087*-OE-N3 and WT plants showed that *IbNAC087* could directly bind to the *IbLOX* and *IbAOS* promoters. The  $\beta$ -*Actin* promoter was used as an internal reference. (F, G) Electrophoretic mobility shift assays (EMSA) analysis of the directive binding of *IbNAC087* to the promoter of *IbLOX* and *IbAOS*, respectively. (H) Dual-luciferase reporter assays in protoplasts showed that *IbNAC087* activated the expression of *IbLOX* and *IbAOS*. Pro35S:*REN* was used as an internal control. Data are presented as the means  $\pm$  SD ( $n = 3$ ). \* and \*\* indicate a significant difference compared with the WT at  $P < 0.05$  and  $P < 0.01$ , respectively, based on Student's *t*-test. Different lowercase letters indicate significant differences ( $P < 0.05$ ; one-way analysis of variance).

were generated from 297 cell aggregates of Lizixiang via *Agrobacterium*-mediated transformation to investigate the role of *IbNIEL* in sweet potato (Figure S15). The *in vitro*-grown *IbNIEL*-OE lines were more sensitive to 86 mmol/L NaCl and 20% PEG6000 stresses than WT plants, with lower FWs and numbers (no.) of main roots (Figure S16; Table S9). The OE-E1, OE-E3, and OE-E4 plants were then planted in transplanting boxes and subjected to 200 mmol/L NaCl or drought

treatment. The *IbNIEL*-OE lines exhibited poor growth than WT under normal conditions, with the average FW and DW decreased by approximately 34% and 44%, respectively. Furthermore, under salt and drought stress, the growth of *IbNIEL*-OE lines was more severely inhibited, with FW and DW decreasing by approximately 72% and 42% under NaCl stress and 73% and 59% under drought stress, respectively (Figure 6A–D; Tables S10, S11). Therefore, the

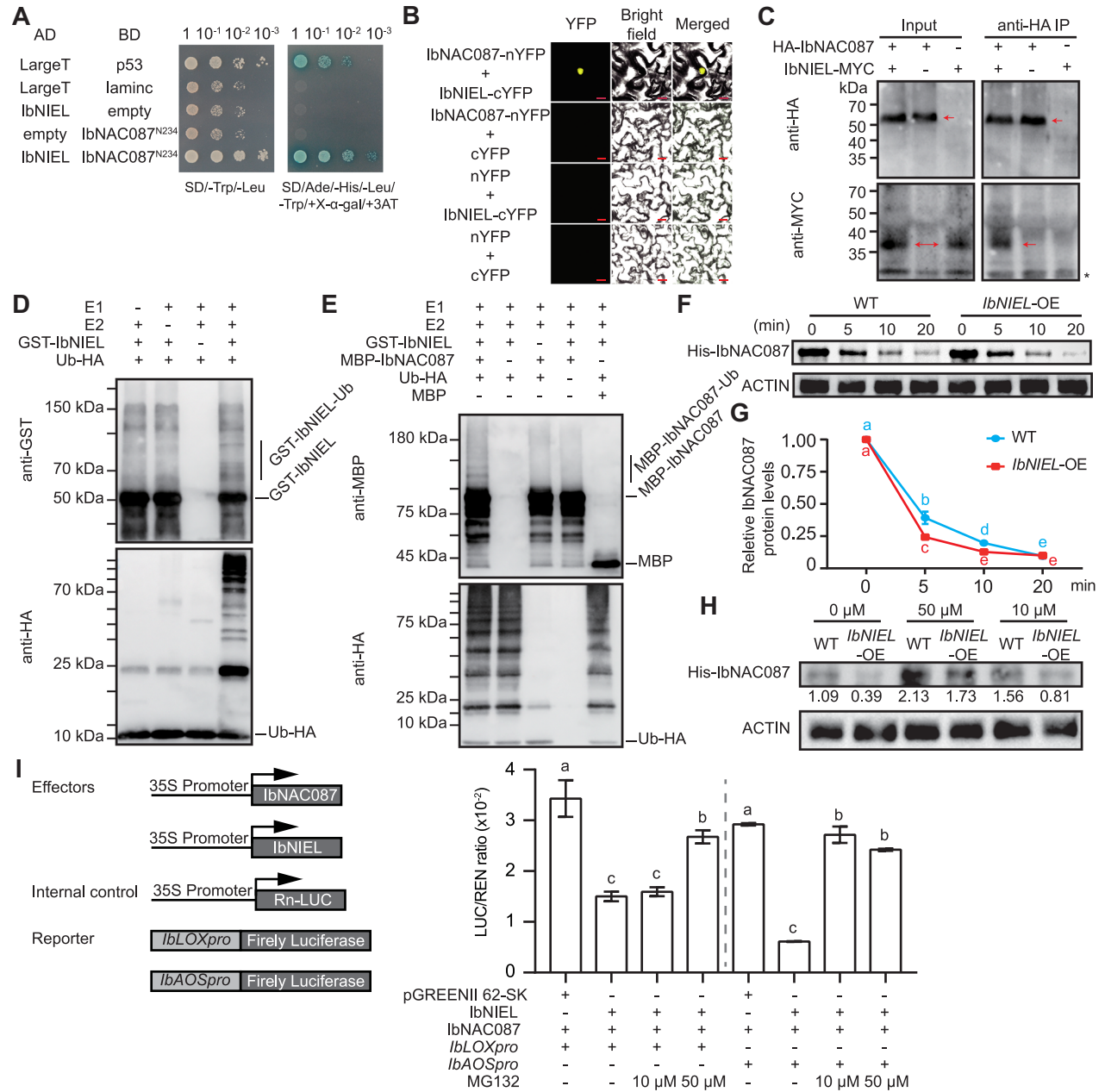


**Figure 5. IbNIEL (NAC087-INTERACTING E3 LIGASE) ubiquitinates IbNAC087 and accelerates its degradation**

(A) IbNIEL interacts with IbNAC087<sup>N234</sup> in yeast. Yeast cells were plated onto synthetic defined (SD)/-Ade/-His/-Leu/-Trp +X-α-gal +3 mmol/L 3AT medium to screen for possible interactions. (B) IbNAC087-nYFP (yellow fluorescent protein) and IbNIEL-cYFP were co-expressed in the nucleus of transformed cells in tobacco leaves. Bars = 20 μm. (C) Co-immunoprecipitation assays showed the association between IbNAC087 and IbNIEL *in vivo*. Total proteins were immuno-precipitated using anti-hemagglutinin (HA) beads and detected with MYC antibody. Red arrow, the interacting protein band; \*, nonspecific protein band. (D) IbNIEL is an active E3 ligase. GST-IbNIEL was tested for E3 ubiquitin ligase activity in the presence and absence of adenosine triphosphate (ATP), ubiquitin, E1, and E2. The protein gel blot was analyzed using anti-glutathione S-transferase (GST) and anti-HA antibodies. (E) IbNIEL ubiquitinates IbNAC087 *in vitro*. Maltose-binding protein (MBP)-IbNAC087 was tested in the presence and absence of ATP, ubiquitin, E1, E2, and GST-IbNIEL. The protein gel blot was analyzed using anti-MBP and anti-HA antibodies. (F, G) IbNIEL promotes the degradation of IbNAC087 *in vivo*. Total proteins extracted from wild-type (WT) and *IbNIEL*-OE-E1 and purified 6His-IbNAC087 protein were incubated, and a Western blot was used for detecting the abundance of IbNAC087. The samples were collected at the indicated time. (H) IbNIEL promoted the degradation of IbNAC087 through the 26S proteasome pathway. Total proteins extracted from WT and *IbNIEL*-OE-E1 and purified 6His-IbNAC087 protein were incubated with 10 μmol/L and 50 μmol/L MG132 treatment, respectively. (I) Dual-luciferase reporter assays in protoplasts showed that IbNIEL inhibited the activation of IbNAC087 on *IbLOX* and *IbAOS*. Pro35S:REN was used as an internal control. Data are presented as the means ± SD (n = 3). Different lowercase letters indicate significant differences (P < 0.05; one-way analysis of variance).

growth of the *IbNIEL-OE* lines was more severely inhibited under salt or drought stress than under normal conditions. The growth and rooting were also weaker in the *IbNIEL-OE* lines than in the WT plants for 7 weeks in a greenhouse without watering (Figure 6E–H). The results indicated that *IbNIEL* negatively regulates salt and drought tolerance in sweet potato.

Endogenous JA levels were significantly lower in *IbNIEL-OE* lines than in WT plants under all salt and drought conditions (Figures S17A, F). The *IbNIEL-OE* lines exhibited lower SOD and POD activities and accumulated more MDA and H<sub>2</sub>O<sub>2</sub> under salt and drought stresses compared with the WT (Figure S17B–E, G–J). Leaf stomata of the *IbNIEL-OE* lines and WT plants were observed after no stress, 200 mmol/L NaCl, 20% PEG, and 20 μmol/L MeJA treatments. Under normal conditions, most stomas in the *IbNIEL-OE* lines and WT plants were partially open. However, under salt and drought stresses, stomas of the *IbNIEL-OE* lines closed more slowly than those of WT plants (Figure S19).

The RT-qPCR assays indicated that the expression of *IbLOX* and *IbAOS* also decreased in the *IbNIEL-OE* plants compared with that in the WT plants (Figure S20A, B, I, J). Additionally, expressions of the ROS scavenging-related genes *IbSOD*, *IbCAT*, *IbAPX*, and *IbPOD*, the ABA biosynthesis-related gene *IbNCED* (Bao et al., 2016), and the photosynthesis-related genes *IbPRK* (Zhang et al., 2019) and *IbCAO* (Yamasato et al., 2005) were significantly lower in the *IbNIEL-OE* lines than in the WT plants under salt and drought stresses (Figure S20C–H, K–P). The results demonstrated that *IbNIEL* reduces salt and drought tolerance by inhibiting *IbNAC087*-mediated JA-dependent ROS scavenging and stomatal closure in sweet potato.

A working model was proposed for this study based on the results obtained above (Figure 7). Abiotic stresses trigger the reduced transcription of *IbNIEL*, resulting in the weakened degradation of *IbNAC087*, mediated and promoted by *IbNIEL*. *IbNAC087* directly targets and activates *IbLOX* and *IbAOS* expressions and promotes JA biosynthesis. Increased JA content triggers a ROS scavenging system and stomatal closure to improve salt and drought stress tolerances in sweet potato. Our results provide a novel regulatory mechanism underlying the *IbNIEL-IbNAC087* module regulating JA-dependent salt and drought responses in sweet potato.

## DISCUSSION

Soil salinity and drought cause metabolic and osmotic damage and repress crop cell growth and yield. Plants have accordingly established efficient mechanisms to cope with such stressful environments (Umezawa et al., 2006; Shinozaki and Yamaguchi-Shinozaki, 2007). The importance of JA signaling in adapting plants to abiotic stress is well documented (Clarke et al., 2009; Liu et al., 2012; Xing et al., 2020; Gao et al., 2022). Although the remarkable JA-rich sweet potato line ND98 possesses superior salt tolerance,

the underlying mechanisms have not yet been elucidated (Zhang et al., 2017a, 2017b). In this study, *IbNAC087*, which was commonly upregulated in multiple salt- and drought-tolerant germplasms, was cloned from ND98. It promotes JA-dependent salt and drought tolerance by directly binding to the promoters of the JA biosynthesis-related genes *IbLOX* and *IbAOS* and activating their expression.

As a key regulator of plant adaptations, JA acts as a signaling molecule that regulates the antioxidant defense system (Su et al., 2021; Esmailzadeh et al., 2022), stomatal closure (Raghavendra and Reddy, 1987; Evans, 2003; Xu et al., 2022), and osmotic adjustment (Abouelsaad and Renault, 2018) in response to abiotic stresses. *AtLOX6* is responsible and essential for stress-induced jasmonate accumulation in roots, and loss-of-function mutants of *LOX6* were more attractive to a detritivorous crustacean and more sensitive to drought (Grebner et al., 2013). JA-deficient mutant *defenseless-1 (def-1)* in tomato had lower activity of enzymatic and nonenzymatic antioxidants under salt stress than WT plants (Abouelsaad and Renault, 2018). *ZmEREB57* in maize increases salt tolerance by directly binding to *ZmAOC2* to activate JA signaling (Zhu et al., 2023). The key JA signaling gene, *SIMYC2*, regulates ROS levels in guard cells and promotes stomatal closure (Xu et al., 2022). In the JA-rich salt-tolerant sweet potato line ND98, stomatal closure and ion homeostasis were maintained under salt stress (Zhang et al., 2017a, 2017b). In this study, the expression of *IbNAC087* increased significantly under MeJA treatment in ND98 (Figure 1E). Under salt and drought stresses, *IbNAC087-OE* plants exhibited significant increases in JA content, whereas the opposite phenotypes were observed in *IbNAC087-Ri* plants (Figure 3D). Exogenous MeJA application effectively promoted stomatal closure and enhanced ROS scavenging in *IbNAC087-OE* plants (Figure S10; Table S5). JA biosynthesis-related genes *IbLOX* and *IbAOS* were targeted directly by *IbNAC087* and proved to be positive regulators against salt and drought tolerance in sweet potato (Figures 4, S12).

NAC TFs play an important regulatory role in plant growth and development and also regulate plant stress responses under adverse conditions, including abiotic stress tolerance (Zheng et al., 2012; Hu et al., 2019; Shang et al., 2020). *SNAC1* increases drought tolerance in rice by increasing root development and decreasing the transpiration rate (Hu et al., 2006; You et al., 2013; Liu et al., 2014; Chen et al., 2023). *TaNAC29* in wheat regulates salt stress tolerance by activating the antioxidant system, which decreases H<sub>2</sub>O<sub>2</sub> accumulation and membrane damage (Xu et al., 2015). *SINAM3* in tomato confers cold tolerance by increasing ethylene production (Dong et al., 2022). Overexpression of *VaNAC26* in *Arabidopsis* improves drought tolerance by promoting JA biosynthesis (Fang et al., 2016). The NAC protein family consists of a conserved NAC domain at the N-terminus, usually divided into five subdomains (A–E) and a highly variable transcriptional region at the C-terminus (Puranik et al., 2012). Limited reports have described the sequence

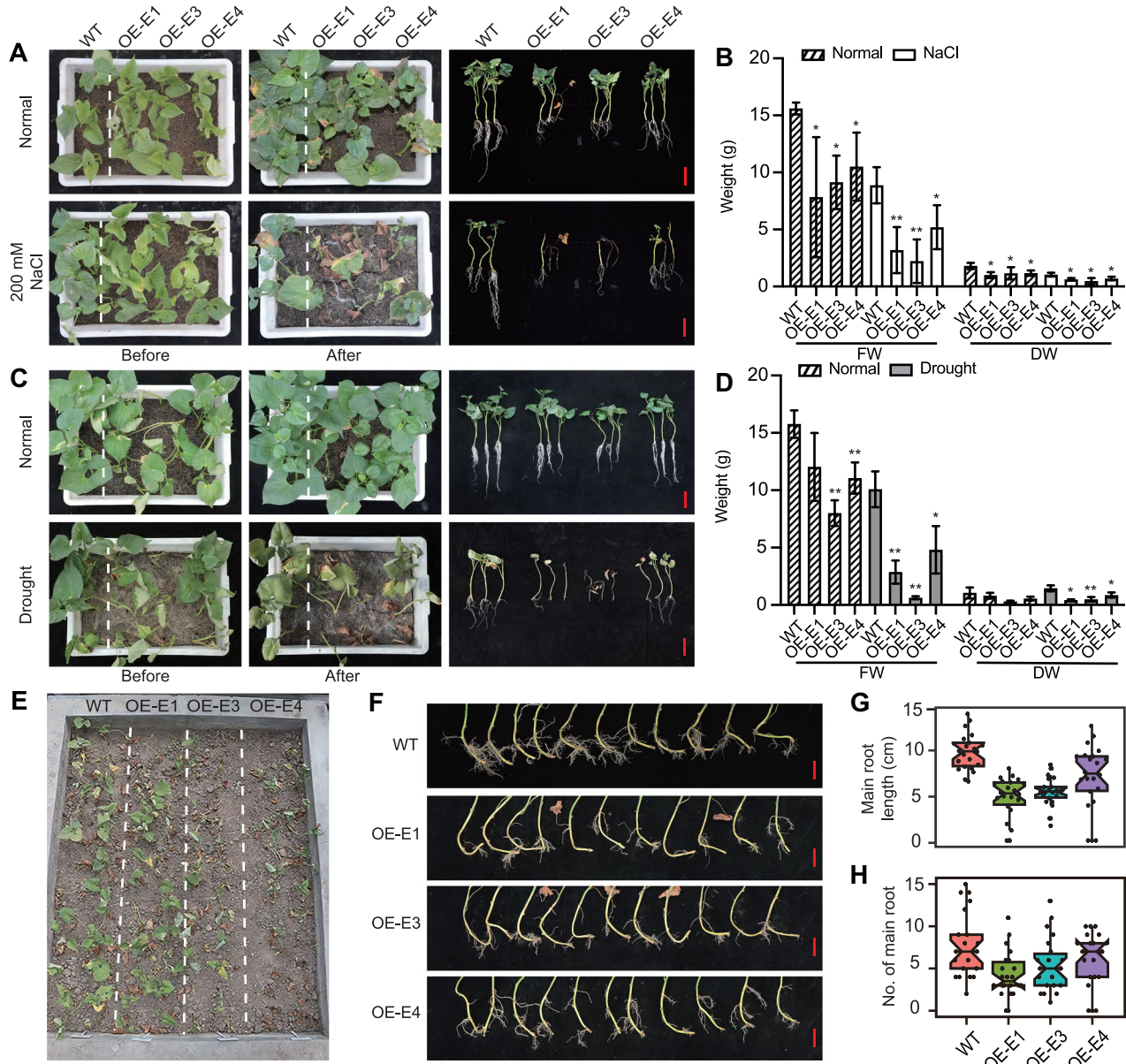


**Figure 6. *IbNIEL* reduces salt and drought tolerance in sweet potato**

(A, B) Phenotypes and fresh weight (FW), dry weight (DW) of *IbNIEL*-OE (overexpression) and wild-type (WT) grown in transplanting boxes without stress or with 200 mmol/L NaCl treatment. Bars = 10 cm. (C, D) Responses and FW, DW of *IbNIEL*-OE and the WT grown in transplanting boxes without stress or with drought treatment. Bars = 10 cm. (E) Responses of 3-month-old field-grown *IbNIEL* transgenic and WT plants (separated by white dotted lines) grown for 7 weeks in greenhouse without watering. (F–H) The rooting of *IbNIEL*-OE and WT grown in a dry pond. Bars = 5 cm. The phenotypes are shown after long-term salt treatment for 6 weeks, drought treatment for 7 weeks in box and dry pond. Time-course phenotypes of *IbNIEL* transgenic and WT plants grown in transplanting boxes under abiotic stresses are shown in Figure S18. Data are presented as the means ± SD ( $n = 3$ ). \* and \*\* indicate a significant difference compared with the WT at  $P < 0.05$  and  $P < 0.01$ , respectively, based on Student's  $t$ -test.

differentiation of NAC proteins in plants. Our data indicated that homologs of NAC087 cluster separately in monocots and dicots, and *IbNAC087* has a high homology with its homologs in dicots (Figure S2). The A and D subdomains of NAC087 homologs showed higher conservation, while differentiation was observed in the B, C, and E subdomains between monocots and dicots, especially in E (Figure S3). Moreover, the C-terminus of the NAC087 homologs

displayed significant diversity in both monocots and dicots (Figure S3). It is speculated that the differentiation of subdomains B, C, and E and the C-terminus might contribute to the functional diversification of NAC proteins in different species.

Additionally, the C-terminus sequences of NAC proteins lack known domains. Still, they are rich in repeats of some simple amino acids (serine-S, threonine-T, proline-P, and STP

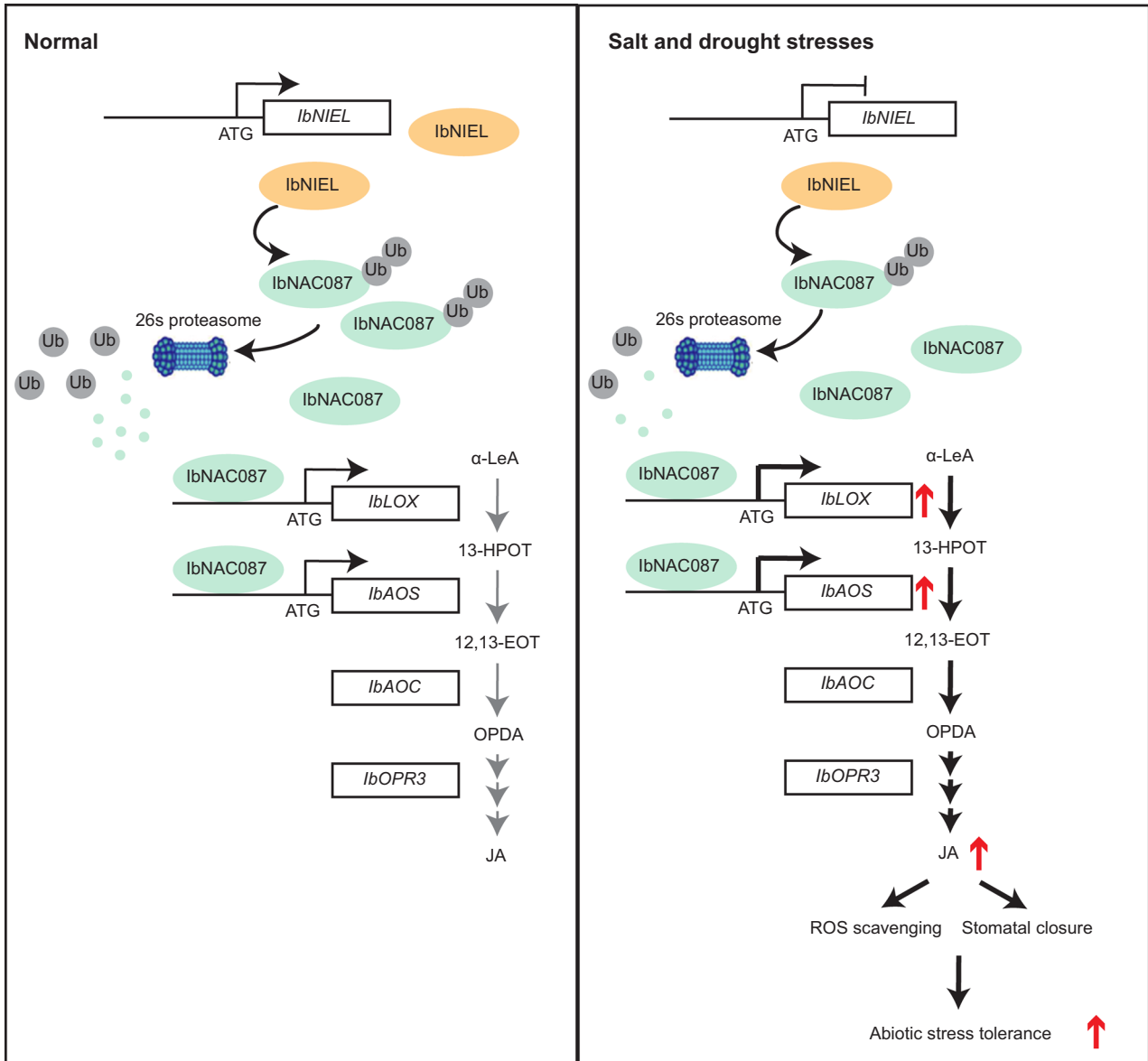


**Figure 7. Proposed working model of the IbNIEL (NAC087-INTERACTING E3 LIGASE)-IbNAC087 regulatory mechanism of abiotic stress response in sweet potato (*Ipomoea batatas*)**

Under normal conditions, IbNAC087 physically interacts with IbNIEL. IbNIEL ubiquitinates the IbNAC087 and accelerates its degradation by 26S proteasome. Under abiotic stresses, the transcription of *IbNIEL* is reduced, resulting in the weakened degradation of IbNAC087. IbNAC087 directly binds on the *IbLOX* and *IbAOS* promoters to activate their transcription and promote jasmonic acid (JA) biosynthesis. Increased JA content triggers reactive oxygen species (ROS) scavenging system and stomatal closure to improve salt and drought stress tolerances in sweet potato. In conclusion, *IbNAC087* is a major positive regulator of abiotic stress response in sweet potato.

cluster) or acidic amino acid residues (glutamic acid-E, aspartic acid-D), which are typical characteristics of transcriptional regions (Künzler et al., 1994; Bobb et al., 1995; Fang et al., 2008). The highly variable transcriptional regions at the C-terminus are critical for diversifying NAC protein functions (Tran et al., 2004; Yamaguchi et al., 2010). Consistent with this, *IbNAC087*<sup>C84</sup>, which is crucial for the transactivation activity of IbNAC087 (Figure 2E), was found to be abundant in the STP cluster (23/84) and acidic residues (11/84) (Table S2). Therefore, *IbNAC087* directly activated *IbLOX* and *IbAOS* to

promote JA-signaling-mediated ROS scavenging and stomatal closure under abiotic stresses.

The RING-type E3 ubiquitin ligases target specific substrates participating in abiotic stress responses. AtPUB11 in *Arabidopsis* negatively regulates drought tolerance by destabilizing LRR1 and KIN7 kinases, which regulate ABA- and drought-promoted stomatal closures (Chen et al., 2021). AtSRAS1.1 mediates the 26S proteasome-dependent degradation of CSN5A, whereas the truncated isoform SRAS1.2 protects CSN5A by competing with

SRAS1.1 in normal conditions to balance plant development and salt tolerance (Zhou et al., 2021). PaIPUB79 in populus regulates ABA-dependent drought tolerance by mediating the degradation of PaWRKY77 and weakening its inhibitory effect on PaIRD26 (Tong et al., 2021). OsRINGzf1 in rice, a RING-H2-type E3 ligase, positively regulates drought tolerance by modulating the ubiquitin-proteasome system (UPS)-dependent degradation of OsPIP2;1 to reduce water loss (Chen et al., 2022). In this study, a RING-type E3 ubiquitin ligase, IbNIEL, ubiquitinated IbNAC087 and accelerated its degradation via the 26S proteasome (Figure 5E–H). IbNIEL interfered with the activation mediated by IbNAC087 on *IbLOX* and *IbAOS* (Figure 5I). Overexpression of *IbNIEL* reduced salt and drought tolerance by inhibiting *IbNAC087*-mediated JA-dependent ROS scavenging and stomatal closure in sweet potato (Figures 6, S17–S20). For future germplasm improvement, repressing the expression of *IbNIEL* in abiotic stress-sensitive germplasms may enable activation of the JA-dependent abiotic stress tolerance of sweet potato.

In summary, this study highlights the beneficial role of *IbNAC087* in increasing tolerance in sweet potato to salt and drought stresses. We also uncovered the transcriptional and post-transcriptional modification regulation mechanisms of the IbNIEL-IbNAC087 module, which induced JA-mediated ROS scavenging and stomatal closure in response to salt and drought stresses in sweet potato. The findings also suggest candidate genes to explore in improving abiotic stress tolerance in crops.

## MATERIALS AND METHODS

### Plant materials and growth conditions

The salt-tolerant sweet potato (*Ipomoea batatas* (L.) Lam.) line ND98 (Zhang et al., 2017a, 2017b) was used in the study, and the salt-sensitive sweet potato variety Lizixiang was used as the WT. The ND98 was used for cloning *IbNAC087*, *IbLOX*, *IbAOS*, and *IbNIEL*, and the Lizixiang was used to characterize the functions of *IbNAC087* and *IbNIEL*. *In vitro*-grown transgenic sweet potato, ND98, and Lizixiang plants were cultured on Murashige and Skoog (MS) medium at 27°C ± 1°C under a photoperiod consisting of 13 h of cool-white fluorescent light (2,000 lx) and 11 h of darkness.

### Gene identification

The RNA sequencing (RNA-seq) data of ND98\_Salt 24 h versus 0 h, Xu22\_Salt versus CK, and *I. triloba*\_Drought 12 h versus 0 h were downloaded from previous studies (Zhang et al., 2017b; Yang et al., 2018; Meng et al., 2020). The false discovery rate (FDR) was used to determine the threshold of the *P*-value in multiple tests; a threshold of FDR < 0.05 according to DESeq. 2 (Love et al., 2014) was considered to indicate differential expression. Heat maps were constructed using the TBtools software (v.1.098696) (Chen et al., 2020).

### Sequence isolation and phylogenetic analysis

Total RNA was extracted from fresh leaves of ND98 using an RNAprep Pure Plant Kit (Tiangen Biotech, Beijing, China), and first-strand complementary DNA (cDNA) synthesis was performed using a PrimeScript™ II 1st Strand cDNA Synthesis Kit (TaKaRa, Tokyo, Japan). Genomic DNA was extracted from fresh leaves of ND98 plants using an EasyPure Plant Genomic DNA Kit (TransGen, Beijing, China). The exon–intron structure was constructed using GSDS2.0 (<http://gsds.gao-lab.org/>). The MW and pI of IbNAC087 were calculated with ExpASY ([https://web.expasy.org/compute\\_pi/](https://web.expasy.org/compute_pi/)). The conserved domains were searched using CD-SEARCH (<https://www.ncbi.nlm.nih.gov/Structure/cdd/wrpsb.cgi>). Phylogenetic analysis was performed using the neighbor-joining method in MEGA X with 1,000 bootstrap iterations (Kumar et al., 2018). Multiple sequence alignments were conducted using DNAMAN 9.0 software (LynnonBioSoft, San Ramon, CA, USA). Genomic structure was analyzed using the SPLIGN program (<https://www.ncbi.nlm.nih.gov/sutils/splign>). PlantCARE (<http://bioinformatics.psb.ugent.be/webtools/plantcare/html/>) was applied to analyze the *cis*-elements in promoter regions (Lescot et al., 2002).

### Activity assessment of IbNAC087 and IbNIEL in *Escherichia coli* and recombinant protein purification

The coding sequence of *IbNAC087* was amplified by PCR using the primer pairs (pETM40-IbNAC087-F/R and pET28a-IbNAC087-F/R) (Table S12) and inserted into pETM40 (*NcoI* and *SalI* sites) and pET28a (*Bam*HI and *Eco*RI sites) vectors, respectively, to produce MBP/His-tagged fusion constructs. The coding sequence of *IbNIEL* was amplified by PCR and inserted into a pGEX6P-1 vector (*Bam*HI and *Eco*RI sites) to produce GST-tagged fusion constructs. The pETM40-IbNAC087, pET28a-IbNAC087, and pGEX6P-1-IbNIEL were introduced into *E. coli* strain Transetta (DE3) cells to produce MBP-IbNAC087, His-IbNAC087, and GST-IbNIEL proteins.

### Expression analysis

Total RNA was extracted from leaf, stem, petiole, fibrous root, pencil root, and storage root tissues of 3-month-old field-grown ND98 plants or leaves of 4-week-old *in vitro*-grown ND98 plants treated with 200 mmol/L NaCl, 20% PEG6000, or 100 μmol/L MeJA in half-Hoagland solution. Experiments were conducted with three biological replicates, each with three plants. Transcript abundances were determined using RT-qPCR (ZF502; ZOMANBIO, Beijing, China). The expressions of *IbNAC087* and *IbNIEL* were measured, and the sweet potato *β-actin* (AY905538) gene was used as the internal control (Table S12). Gene expression was quantified using the comparative cycle threshold (*C<sub>T</sub>*) method (Schmittgen and Livak, 2008).

### Promoter expression analysis

The promoter of *IbNAC087* was inserted into the *PacI* and *AscI* sites of the expression vector pMDC 162 (Table S12). As previously described, the pMDC162-IbNAC087pro plasmid was transformed into Lizixiang via *Agrobacterium*

*tumefaciens*-mediated transformation (Zhang et al., 2022). The expression of *gusA* was determined in the leaves, stems, and roots of *in vitro*-grown transgenic sweet potato. Four-week-old *in vitro*-grown transgenic sweet potato plants were cultured separately in half-strength Hoagland solution with 200 mmol/L NaCl, 20% PEG6000, or 100  $\mu$ mol/L MeJA for 0.5, 3, 12, and 48 h. The expression of *gusA* was determined using RT-qPCR and the comparative  $C_T$  method (Schmittgen and Livak, 2008). The sweet potato  $\beta$ -actin (AY905538) gene was used as the internal control (Table S12).

### Subcellular localization

The encoding regions of *IbNAC087* and *IbNIEL* without the stop codon were amplified as primer pairs (1300-IbNAC087-GFP-F/R or 1300-IbNIEL-GFP-F/R) and integrated into *KpnI* and *SalI* sites of the expression vector pCAMBIA1300-GFP (Table S12) driven by the cauliflower mosaic virus (CaMV) 35S promoter to produce *IbNAC087*-GFP and *IbNIEL*-GFP fusion constructs. Recombinant vectors *p35S:IbNAC087-GFP*, *p35S:IbNIEL-GFP*, *p35S:GFP* (as the control), and the PIP2A-mCherry (membrane marker) were transformed into *A. tumefaciens* strain EHA105 using the heat shock method. Isolation of rice protoplasts and transfection of vectors into protoplasts were conducted, as previously described (Liu et al., 2021). The fusion constructs were transfected into isolated protoplasts. Protoplasts were resuspended in WI solution for 16 h in the dark after transient transfection. The GFP fluorescent signals were observed with an LSM880 microscope (Zeiss, Oberkochen, Germany) with an argon laser (488 nm excitation wavelength).

### Transcriptional activation assay

A transcriptional activation assay was conducted according to the Yeast Protocols Handbook (Clontech, Mountain View, CA, USA). The full-length, 1-32 N-terminal amino acid residues, 1-234 N-terminal amino acid residues, and 235-318 C-terminal amino acid residues of *IbNAC087* were amplified by PCR using the primer pairs (pGBKT7-IbNAC087-F/R, pGBKT7-IbNAC087-F/-R32, pGBKT7-IbNAC087-F/R234 and pGBKT7-IbNAC087-FC/RC) (Table S12). These amplified regions were then cloned into the *NdeI* and *EcoRI* sites of the pGBKT7 vector (Invitrogen) to produce pGBKT7-IbNAC087<sup>N32</sup>, pGBKT7-IbNAC087<sup>N234</sup> and pGBKT7-IbNAC087<sup>C84</sup> constructs. The pGBKT7-IbNAC087<sup>N32</sup>, pGBKT7-IbNAC087<sup>N234</sup>, and pGBKT7-IbNAC087<sup>C84</sup> constructs were transformed into the Y2H gold yeast strain using the PEG/LiAc method. An empty pGBKT7 vector was used as a negative control (N), whereas pGBKT7-53 was used as a positive control (P). The transformed yeast strains were screened on synthetic defined (SD) plates without tryptophan (SD/-Trp) and then transferred to SD medium lacking tryptophan/histidine/adenine (SD/-Trp/-His/-Ade/X- $\alpha$ -gal) to observe yeast growth at 30°C for 2–3 d.

### Production of transgenic sweet potato plants

The coding region of *IbNAC087* was amplified by PCR using the primer pairs (pCM1307-IbNAC087-F/R) (Table S12) and

inserted into the *SalI* and *XbaI* sites of the plant expression vector pCM1307 to produce the *p35S:IbNAC087-HA* fusion construct. A pair of forward and reverse nonconserved fragments of *IbNAC087* were inserted into the plant RNA interference (RNAi) vector pCAMBIA1300-35SI-X to generate *35SI-X-IbNAC087* constructs. The *p35S:IbNAC087-HA*, *35SI-X-IbNAC087*, and *p35S:IbNIEL-GFP* constructs were separately transfected into *A. tumefaciens* strain EHA105 by the heat shock method. As previously described, transformation and plant regeneration were performed using embryogenic suspension cultures of the Lizixiang (Zhang et al., 2022). Putative transgenic sweet potato plants were identified by PCR analysis with identifying primers and RT-qPCR analysis (Table S12). Transgenic and WT plants were transferred to soils in a greenhouse and then to the field for evaluation. Cuttings approximately 25 cm in length were used for further functional analysis, as previously described (Zhang et al., 2019).

The coding regions of *IbLOX* and *IbAOS* were amplified by PCR using the primer pairs (pCM1307-IbLOX-F/R and pCM1307-IbAOS-F/R) (Table S12) and inserted into the *SalI* and *XbaI* sites of plant expression vector pCM1307 to produce the *p35S:IbLOX-HA* and *p35S:IbAOS-HA* fusion constructs, and subsequently transfected into *A. tumefaciens* strain EHA105 to infect Lizixiang as previously described (Cao et al., 2022). The inoculated plants were incubated in the transplantation box for 7 d and then challenged with NaCl and PEG stresses. Six plants from each gene were used.

### Assays for salt and drought tolerance

*In vitro*-grown *IbNAC087*-OE, *IbNIEL*-OE, and WT sweet potato plants were treated separately on MS medium supplemented with 200 mmol/L NaCl or 86 mmol/L NaCl and 20% PEG6000. After 4 weeks, growth and rooting were observed. Staining with 3,30-diaminobenzidine (DAB) and nitro blue tetrazolium (NBT) was performed as previously described (Zhang et al., 2022). The contents of H<sub>2</sub>O<sub>2</sub> and MDA and the SOD and CAT activities were measured using assay kits (Comin Biotechnology Co. Ltd, Suzhou, China). Three plants from each line were used.

Cuttings approximately 25 cm in length from field-grown transgenic and WT sweet potato plants were planted in a transplanting box in a glasshouse and irrigated with half-strength Hoagland solution for 2 weeks. For salt and drought tolerance assays, each plant was irrigated with 300 mL of 200 mmol/L NaCl solution once every 3 d or was drought-stressed. Three cuttings from each line were treated. FW and DW were immediately measured. The JA content (Ruixinbio, Quanzhou, China), H<sub>2</sub>O<sub>2</sub> and MDA content, and SOD, POD, and CAT enzyme activities in the leaves of transgenic and WT plants were measured using assay kits (Comin Biotechnology Co. Ltd). Three plants from each line were used.

Cuttings approximately 25 cm in length from field-grown *IbNIEL* transgenic and WT sweet potato plants were planted in a dry pond. Each plant was irrigated with 300 mL of water for 1 week and then drought-stressed (without water)

for 7 weeks. Twenty cuttings from each line were treated. The main root length and number of roots were immediately measured.

### Observation of leaf stoma

Fully unfolded leaves at the same plant position were selected for the stoma observations. The abaxial epidermal stripes of the leaves were peeled away, and the stomas were imaged using Echo Revolve light microscopy (ECHO, San Diego, CA, USA). Stomatal apertures were estimated with ImageJ software (<https://imagej.nih.gov/ij/download.html>), as previously described (Lin et al., 2020). Approximately 100 stomatal pores from the same leaf region were examined for each measurement assay.

### Chromatin immunoprecipitation assay

In brief, the leaves of *IbNAC087*-OE-N3 and WT plants were used in a ChIP assay, according to Zhang et al. (2022). The sample was ground to a powder in liquid nitrogen and subjected to nuclear isolation. Anti-HA (1:1,000, H3663; Sigma; Missouri, USA) antibodies were used to immunoprecipitate the protein-DNA complex and the precipitated DNA was recovered. An equal number of chromatin samples without antibody precipitation was used as an input control. The ChIP DNA was analyzed by qPCR, and the ChIP values were normalized against the values of the respective inputs. The primers used in the ChIP-qPCR are listed in Table S12.

### Yeast one-hybrid assay

The coding sequence of *IbNAC087* was amplified by PCR using the primer pairs (pB42AD-*IbNAC087*-F/R) (Table S12) and inserted into the *EcoRI* and *XhoI* sites of the pB42AD vector to produce pB42AD-*IbNAC087* constructs. In contrast, promoter fragments of *IbLOX* and *IbAOS* were amplified by PCR using the primer pairs (pLacZi2 $\mu$ -*IbLOX/IbAOSpro*-F/R) (Table S12) cloned into the pLacZi2 $\mu$  vector to produce pLacZi2 $\mu$ -*IbLOX/IbAOSpro*. The pB42AD-*IbNAC087* and empty pB42AD vectors were separately transformed into yeast strain EGY48 using the PEG/LiAc method with pLacZi2 $\mu$ -*IbLOXpro/IbAOSpro* constructs. Yeast cells were plated on SD plates without arginine and tryptophan (SD/-Ura/-Trp). Positive clones were transferred to an SD medium lacking arginine and tryptophan (SD/-Ura/-Trp) but containing galactose (20%), raffinose (20%), buffered (BU) salt, and X-gal for stringent screening of possible interactions according to the protocol of the Matchmaker OneHybrid System (Clontech).

### Electrophoretic mobility shift assay

His-*IbNAC087* was purified from *E. coli* strain Transetta (DE3) cells using standard protocols. The DNA probes containing CGT(A/C) were synthesized and labeled with biotin at the 5' end. Unlabeled probes were used as competitors. Biotin probes in which the CGT(A/C) were mutated to AAAA/TTTT were used as mutant probes. Probe sequences are listed in Table S12. The EMSAs were performed using a LightShift Chemiluminescent EMSA Kit (20148; Thermo Scientific,

Waltham, MA, USA) according to the manufacturer's instructions. The experiment was independently repeated three times, with similar results.

### Dual-luciferase assay

For the transcriptional activity assay, 1-234 aa N-terminal amino acid residues and 235-318 aa C-terminal amino acid residues from *IbNAC087* were separately amplified by PCR using the primer pairs (62SK-BD-*IbNAC087*-N234-F/R, 62SK-BD-*IbNAC087*-C-F/R) (Table S12) and inserted into the pGreenII 62-SK-BD as effectors and the pGreenII 0800-LUC vector containing the GAL4 DNA consensus binding site, luciferase (LUC), and renilla luciferase (REN) was used as the reporter.

In the assay of *IbNAC087* activation of *IbLOX* and *IbAOS* promoters, the coding sequence of *IbNAC087* and *IbNIEL* were amplified by PCR using the primer pairs (62SK-*IbNAC087*-F/R, 62SK-*IbNIEL*-F/R) (Table S12) and cloned into the *PstI* and *EcoRI* sites of the pGreenII 62-SK vector, which was used as effectors. The *IbLOX* and *IbAOS* promoters (*KpnI* and *PstI* sites) were amplified using PCR with the primer pairs (0800-*IbLOX/IbAOSpro*-F/R) (Table S12) and inserted upstream of LUC into the pGreenII 0800-LUC vector to generate the *IbLOX/IbAOSpro*:LUC reporter construct, which were used as reporters. Rice protoplasts were isolated and used for dual-LUC assays, as previously described (Liu et al., 2021), and were incubated overnight with 10  $\mu$ mol/L and 50  $\mu$ mol/L MG132, respectively. Firefly LUC and REN activity levels were measured using a Dual-Luciferase Reporter Assay System (E1910; Promega, Madison, WI, USA). Luciferase activity was normalized to REN activity. Three biological replicates were analyzed. The experiment was independently repeated three times, with similar results.

### Yeast two-hybrid assay

Yeast two-hybrid assays were performed, as described in the Yeast Protocols Handbook (Clontech). The coding sequence of *IbNIEL* was amplified by PCR (Table S12) and cloned into pGADT7. Constructs pGBKT7-*IbNAC087*<sup>N234</sup> and pGADT7-*IbNIEL* were introduced into the yeast strain Y2H gold using the lithium acetate method. Yeast cells were plated onto an SD medium lacking leucine and tryptophan (SD/-Leu/-Trp) and transferred to an SD medium lacking adenine, histidine, leucine, and tryptophan (SD/-Ade/-His/-Leu/-Trp) and containing 3 mmol/L 3-aminotriazole (3-AT) and X- $\alpha$ -gal for stringent screening of interactions. The experiment was independently repeated three times, with similar results.

### Bimolecular fluorescence complementation

The coding sequence of *IbNAC087* was amplified by PCR using the primer pairs (BiFC-*IbNAC087*-F/R) (Table S12) and cloned into the *Ascl* and *KpnI* sites of the pSPYCE-35S vector harboring the coding sequence for the N-terminal half of the YFP; *IbNIEL* was amplified by PCR using the primer pairs (BiFC-*IbNIEL*-F/R) (Table S12) and cloned into the *Ascl* and *KpnI* sites of pSPYNE-35S vector encoding the

## IbNAC087 regulates abiotic stress response

C-terminal half of YFP (Walter et al., 2004). The pSPYCE-35S:*IbNAC087-nYFP* and pSPYCE-35S:*IbNIEL-cYFP* vectors were transformed into *A. tumefaciens* strain EHA105 and coinjected into *N. benthamiana* leaves (Batoko et al., 2000). After 48 h of growth, yellow fluorescence was observed under a confocal laser-scanning microscope (LSM880; Zeiss) with an argon laser (514 nm excitation wavelength). The experiment was independently repeated three times, with similar results.

**Co-immunoprecipitation assay**

The p35S:*IbNAC087-HA* and p35S:*IbNIEL-MYC* constructs were transiently transformed into *N. benthamiana* leaf epidermal cells using *A. tumefaciens* infiltration (Batoko et al., 2000). Total protein samples extracted from the leaves of *N. benthamiana* were tagged with MYC and HA in a Co-IP buffer. Protein extracts were mixed with HA agarose beads (B26201; Bimake, Houston, TX, USA) and incubated at 4°C for 2 h. After at least five washes, the agarose beads were recovered and mixed with sodium dodecyl sulfate sample buffer. Samples were detected by immunoblotting using anti-MYC (1:5,000, M4439; Sigma) and anti-HA (1:5,000, H3663; Sigma) antibodies. Horseradish peroxidase-conjugated rabbit anti-mouse immunoglobulin G (H + L) (1:20,000, 31450; Thermo Fisher, Waltham, MA, USA) antibody was used as the secondary antibody. Three biological replicates from different plants were analyzed. The experiment was independently repeated three times, with similar results.

**In vitro ubiquitination assay**

An *in vitro* ubiquitination assay was performed as previously described (Chen et al., 2021) with minor modifications. His-Ub-HA, GST-IbNIEL, and MBP-IbNAC087 were purified from *E. coli* BL21 (DE3) cell cultures using standard protocols. The UBE1 (UBE-024; Ubbiotech, Changchun, China) and UBE2D2 (UBE-622; Ubbiotech) enzymes and the ATP-Mg buffer (UBE-001; Ubbiotech) were used in the study. One microgram of MBP-IbNAC087 and 1.0 µg of GST-IbNIEL recombinant proteins were incubated at 37°C for 2 h in the presence or absence of 0.5 µg of UBE1, 1.5 µg of UBE2D2, and 2.5 µg of Ub. Anti-GST (1:5,000, 05-782; Sigma) and anti-HA (1:5,000, H3663; Sigma) antibodies were used to detect the self-ubiquitination of IbNIEL. Anti-MBP (1:5,000, M1001; Lablead, Beijing, China) and anti-HA (1:5,000, H3663; Sigma) antibodies were used to detect the ubiquitination of IbNAC087 by IbNIEL.

**Cell-free degradation assay**

Cell-free degradation assays were performed as previously described (Lv et al., 2014), with minor modifications. Total proteins were extracted from the leaves of the WT and *IbNIEL*-OE plants and adjusted to equal concentrations in the degradation buffer for each assay. The purified proteins of His-IbNAC087 were incubated with various protein extracts at 25°C for 0, 5, 10, and 20 min. In addition, His-IbNAC087 was incubated with multiple protein extracts at 25°C for 20 min with or without MG132 treatment. The His-IbNAC087

protein was detected with diluted anti-His antibody (1:1,000, AF2876; Beyotime, Shanghai, China). Quantitative analysis of immunoblots was performed using the Quantity Tools of Image Lab software (Bio-Rad).

**Accession numbers**

Sequence data from this article can be found in the Sweetpotato GARDEN (Sweetpotato Genome and Resource Database ENtry) (<http://sweetpotato-garden.kazusa.or.jp/>) under accession numbers *IbNAC087* (ltr\_sc000462.1\_g00010.1), *IbLOX* (ltr\_sc001012.1\_g00005.1), *IbAOS* (ltr\_sc001275.1\_g00001.1), *IbNIEL* (ltr\_sc000449.1\_g00025.1).

**ACKNOWLEDGEMENTS**

This work was supported by the National Key R&D Program of China (2023YFD1200700/2023YFD1200702), the Beijing Natural Science Foundation (grant no. 6212017), the Beijing Food Crops Innovation Consortium Program (BAIC02-2023), the Project of Sanya Yazhou Bay Science and Technology City (grant no. SCKJ-JYRC-2022-61/SYND-2022-09), and China Agriculture Research System of MOF and MARA (CARS-10, Sweetpotato), and Chinese Universities Scientific Fund (2023TC057/2022TC003).

**CONFLICTS OF INTEREST**

The authors declare no conflict of interest.

**AUTHOR CONTRIBUTIONS**

X.L., Z.W., S.S. performed most of the research and X.L. drafted the manuscript. Z.D., and J.Z. carried out the analysis of transcriptome data. W.W., and K.P. performed some dual-LUC assays. W.G. carried out some analyses of physiological and biochemical indicators. S.X. carried out promoter expression analysis. F.T., N.Z., S.G., Hong Z. and Q.L. revised the manuscript. S.H., and Huan Z. designed the experiments, supervised the study, and revised the manuscript. All authors read and approved of its content.

**Edited by:** Qi Xie, Institute of Genetics and Developmental Biology, CAS, China

**Received** Aug. 12, 2023; **Accepted** Jan. 8, 2024

**OO:** OnlineOpen

**REFERENCES**

- Abouelsaad, I., and Renault, S.** (2018). Enhanced oxidative stress in the jasmonic acid-deficient tomato mutant *def-1* exposed to NaCl stress. *J. Plant Physiol.* **226**: 136–144.
- Ahmadi, F.I., Karimi, K., and Struik, P.C.** (2018). Effect of exogenous application of methyl jasmonate on physiological and biochemical

- characteristics of *Brassica napus* L. cv. Talaye under salinity stress. *S. Afr. J. Bot.* **115**: 5–11.
- Ballas, N., Wong, L.M., and Theologis, A.** (1993). Identification of the auxin-responsive element, AuxRE, in the primary indoleacetic acid-inducible gene, *PS-IAA4/5*, of pea (*Pisum sativum*). *J. Mol. Biol.* **233**: 580–596.
- Bao, G.G., Zhuo, C.L., Qian, C.M., Xiao, T., Guo, Z.F., and Lu, S.Y.** (2016). Co-expression of *NCED* and *ALO* improves vitamin C level and tolerance to drought and chilling in transgenic tobacco and stylo plants. *Plant Biotechnol. J.* **14**: 206–214.
- Bartels, D., and Sunkar, R.** (2005). Drought and salt tolerance in plants. *Crit. Rev. Plant Sci.* **24**: 23–58.
- Batoko, H., Zheng, H.Q., Hawes, C., and Moore, I.** (2000). A rab1 GTPase is required for transport between the endoplasmic reticulum and golgi apparatus and for normal golgi movement in plants. *Plant Cell* **12**: 2201–2218.
- Bi, Y., Wang, H., Yuan, X., Yan, Y.Q., Li, D.Y., and Song, F.M.** (2023). The NAC transcription factor *ONAC083* negatively regulates rice immunity against *Magnaporthe oryzae* by directly activating transcription of the RING-H2 gene *OsRFP2-6*. *J. Integr. Plant Biol.* **65**: 854–875.
- Bobb, A.J., Eiben, H.G., and Bustos, M.M.** (1995). PvAlf, an embryo-specific acidic transcriptional activator enhances gene expression from phaseolin and phytohemagglutinin promoters. *Plant J.* **8**: 331–343.
- Busk, P.K., and Pages, M.** (1997). Protein binding to the abscisic acid-responsive elements is independent of VIVIPROUS1 *in vivo*. *Plant Cell* **9**: 2261–2270.
- Cao, X., Xie, H., Song, M., Lu, J., Ma, P., Huang, B., Wang, M., Tian, Y., Chen, F., Peng, J., et al.** (2022). Cut-dip-budding delivery system enables genetic modifications in plants without tissue culture. *Innovation* **4**: 100345.
- Chen, C., Chen, H., Zhang, Y., Thomas, H.R., Frank, M.H., He, Y., and Xia, R.** (2020). TBtools: An integrative toolkit developed for interactive analyses of big biological data. *Mol. Plant* **13**: 1194–1202.
- Chen, F.H., Zhang, H.M., Li, H., Lian, L., Wei, Y.D., Lin, Y.L., Wang, L.N., He, W., Cai, Q.H., Xie, H.G., et al.** (2023). IPA1 improves drought tolerance by activating SNAC1 in rice. *BMC Plant Biol.* **23**: 55–66.
- Chen, S.J., Xu, K., Kong, D.Y., Wu, L.Y., Chen, Q., Ma, X.S., Ma, S.Q., Li, T.F., Xie, Q., Liu, H.Y., et al.** (2022). Ubiquitin ligase *OsRINGzf1* regulates drought resistance by controlling the turnover of *OsPIP2;1*. *Plant Biotechnol. J.* **20**: 1743–1755.
- Chen, X.X., Wang, T.T., Rehman, A.U., Wang, Y., Qi, J.S., Li, Z., Song, C.P., Wang, B.S., Yang, S.H., and Gong, Z.Z.** (2021). Arabidopsis U-box E3 ubiquitin ligase PUB11 negatively regulates drought tolerance by degrading the receptor-like protein kinases LRR1 and KIN7. *J. Integr. Plant Biol.* **63**: 494–509.
- Clarke, S.M., Cristescu, S.M., Miersch, O., Harren, F.J., Wasternack, C., and Mur, L.A.** (2009). Jasmonates act with salicylic acid to confer basal thermotolerance in *Arabidopsis thaliana*. *New Phytol.* **182**: 175–187.
- Dong, Y.F., Tang, M.J., Huang, Z.L., Song, J.N., Xu, J., Ahammed, G.J., Yu, J.Q., and Zhou, Y.H.** (2022). The miR164a-NAM3 module confers cold tolerance by inducing ethylene production in tomato. *Plant J.* **111**: 440–456.
- Duroux, L., and Welinder, K.G.** (2003). The peroxidase gene family in plants: A phylogenetic overview. *J. Mol. Evol.* **57**: 397–407.
- Ernst, H.A., Olsen, A.N., Larsen, S., and Leggio, L.L.** (2004). Structure of the conserved domain of ANAC, a member of the nac family of transcription factors. *EMBO Rep.* **5**: 297–303.
- Esmailzadeh, S., Fallah, H., Niknejad, Y., Mahmoudi, M., and Tari, D.B.** (2022). Methyl jasmonate increases aluminum tolerance in rice by augmenting the antioxidant defense system, maintaining ion homeostasis, and increasing nonprotein thiol compounds. *Environ. Sci. Pollut. Res. Int.* **29**: 46708–46720.
- Evans, N.H.** (2003). Modulation of guard cell plasma membrane potassium currents by methyl jasmonate. *Plant Physiol.* **131**: 8–11.
- Fang, J.L., Chai, Z., Yao, W., Chen, B.S., and Zhang, M.Q.** (2020). Interactions between ScNAC23 and ScGAI regulate GA-mediated flowering and senescence in sugarcane. *Plant Sci.* **304**: 110806–110817.
- Fang, L.C., Su, L.Y., Sun, X.M., Li, X.B., Sun, M.X., Karungo, S.K., Fang, S., Chu, J.F., Li, S.H., and Xin, H.P.** (2016). Expression of *Vitis amurensis* *NAC26* in *Arabidopsis* enhances drought tolerance by modulating jasmonic acid synthesis. *J. Exp. Bot.* **67**: 2829–2845.
- Fang, Y.J., You, J., Xie, K.B., Xie, W.B., and Xiong, L.Z.** (2008). Systematic sequence analysis and identification of tissue-specific or stress-responsive genes of NAC transcription factor family in rice. *Mol. Genet. Genomics* **280**: 535–546.
- FAO.** (2022). Crops and livestock products. Available from: <https://www.fao.org/faostat/en/#data/QCCL>
- Gao, L.T., Jia, S.Z., Cao, L., Ma, Y.J., Wang, J.L., Lan, D., Guo, G.Y., Chai, J.F., and Bi, C.L.** (2022). An F-box protein from wheat, TaFBA-2A, negatively regulates JA biosynthesis and confers improved salt tolerance and increased JA responsiveness to transgenic rice plants. *Plant Physiol. Biochem.* **182**: 227–239.
- Gao, X.R., Zhang, H., Li, X., Bai, Y.W., Peng, K., Wang, Z., Dai, Z.R., Bian, X.F., Zhang, Q., Jia, L.C., et al.** (2023). The B-box transcription factor IbBBX29 regulates leaf development and flavonoid biosynthesis in sweet potato. *Plant Physiol.* **191**: 496–514.
- Grebner, W., Stingl, N.E., Oenel, A., Mueller, M.J., and Berger, S.** (2013). Lipoxygenase6-dependent oxylipin synthesis in roots is required for abiotic and biotic stress resistance of Arabidopsis. *Plant Physiol.* **161**: 2159–2170.
- Hu, H.H., Dai, M.Q., Yao, J.L., Xiao, B.Z., Li, X.H., Zhang, Q.F., and Xiong, L.Z.** (2006). Overexpressing a NAM, ATAF, and CUC (NAC) transcription factor enhances drought tolerance and salt tolerance in rice. *Proc. Natl. Acad. Sci. U.S.A.* **103**: 12987–12992.
- Hu, P., Zhang, K.M., and Yang, C.P.** (2019). BpNAC012 positively regulates abiotic stress responses and secondary wall biosynthesis. *Plant Physiol.* **179**: 700–717.
- Karkute, S.G., Gujjar, R.S., Rai, A., Akhtar, M., Singh, M., and Singh, B.** (2018). Genome wide expression analysis of WRKY genes in tomato (*Solanum lycopersicum*) under drought stress. *Plant Gene* **13**: 8–17.
- Kazan, K., and Manners, J.M.** (2013). MYC2: The master in action. *Mol. Plant* **6**: 686–703.
- Kim, S.E., Bian, X., Lee, C.J., Park, S.U., Lim, Y.H., Kim, B.H., Park, W.S., Ahn, M.J., Ji, C.Y., Yu, Y., et al.** (2021). Overexpression of 4-hydroxyphenylpyruvate dioxygenase (*IbHPPD*) increases abiotic stress tolerance in transgenic sweetpotato plants. *Plant Physiol. Biochem.* **167**: 420–429.
- Kumar, S., Stecher, G., Li, M., Knyaz, C., and Tamura, K.** (2018). MEGA X: Molecular evolutionary genetics analysis across computing platforms. *Mol. Biol. Evol.* **35**: 1547–1549.
- Kuo, H.Y., Kang, F.C., and Wang, Y.Y.** (2020). Glucosinolate Transporter1 involves in salt-induced jasmonate signaling and alleviates the repression of lateral root growth by salt in *Arabidopsis*. *Plant Sci.* **297**: 110487.
- Künzler, M., Braus, G.H., Georgiev, O., Seipel, K., and Schaffner, W.** (1994). Functional differences between mammalian transcription activation domains at the yeast *GAL1* promoter. *EMBO J.* **13**: 641–645.
- Lescot, M., Déhais, P., Thijs, G., Marchal, K., Moreau, Y., Van de Peer, Y., Rouzé, P., and Rombauts, S.** (2002). PlantCARE, a database of plant cis-acting regulatory elements and a portal to tools for *in silico* analysis of promoter sequences. *Nucleic Acids Res.* **30**: 325–327.
- Li, T.M., Cheng, X., Wang, X.W., Li, G.G., Wang, B.B., Wang, W.Y., Zhang, N., Han, Y.L., Jiao, B.L., Wang, Y.J., et al.** (2021). Glyoxalase I-4 functions downstream of NAC72 to modulate downy mildew resistance in grapevine. *Plant J.* **108**: 394–410.

- Lin, Q.F., Wang, S., Dao, Y.H., Wang, J.Y., and Wang, K. (2020). *Arabidopsis thaliana* trehalose-6-phosphate phosphatase gene *TPPI* enhances drought tolerance by regulating stomatal apertures. *J. Exp. Bot.* **71**: 4285–4297.
- Liu, G.Z., Li, X.L., Jin, S.X., Liu, X.Y., Zhu, L.F., Nie, Y.C., and Zhang, X.L. (2014). Overexpression of rice NAC gene *SNAC1* improves drought and salt tolerance by enhancing root development and reducing transpiration rate in transgenic cotton. *PLoS ONE* **9**: e86895.
- Liu, H., Dong, S.Y., Li, M., Gu, F.W., Yang, G.L., Guo, T., Chen, Z.Q., and Wang, J.F. (2021). The class III peroxidase gene *OsPRX30*, transcriptionally modulated by the AT-hook protein *OsATH1*, mediates rice bacterial blight-induced ROS accumulation. *J. Integr. Plant Biol.* **63**: 393–408.
- Liu, X., Chi, H., Yue, M., Zhang, X., Li, W., and Jia, E. (2012). The regulation of exogenous jasmonic acid on UV-b stress tolerance in wheat. *J. Plant Growth Regul.* **31**: 436–447.
- Liu, Y.F., Liu, Y., Chen, Q.M., Yin, F.L., Song, M.B., Cai, W., and Shuai, L. (2023). Methyl jasmonate treatment alleviates chilling injury and improves antioxidant system of okra pod during cold storage. *Food Sci. Nutr.* **11**: 2049–2060.
- Love, M.I., Huber, W., and Anders, S. (2014). Moderated estimation of fold change and dispersion for RNA-seq data with DESeq. 2. *Genome Biol.* **15**: 550.
- Lv, Q.D., Zhong, Y.J., Wang, Y.G., Wang, Z.Y., Zhang, L., Shi, J., Wu, Z.C., Liu, Y., Mao, C.Z., Yi, K.K., et al. (2014). SPX4 negatively regulates phosphate signaling and homeostasis through its interaction with PHR2 in rice. *Plant Cell* **26**: 1586–1587.
- Ma, B.J., Liu, X.F., Guo, S.Y., Xie, X.L., Zhang, J., Wang, J.Y., Zheng, L.L., and Wang, Y.C. (2021). RtnAC100 involved in the regulation of ROS, Na<sup>+</sup> accumulation and induced salt-related PCD through MeJA signal pathways in recetohalophyte *Reaumuria trigyna*. *Plant Sci.* **310**: 110976.
- Mao, C.J., He, J.M., Liu, L.N., Deng, Q.M., Yao, X.F., Liu, C.M., Qiao, Y.L., Li, P., and Ming, F. (2020). OsNAC2 integrates auxin and cytokinin pathways to modulate rice root development. *Plant Biotechnol. J.* **18**: 429–442.
- Mao, C.J., Lu, S.C., Lv, B., Zhang, B., Shen, J.B., He, J.M., Luo, L.Q., Xi, D.D., Chen, X., and Ming, F. (2017). A rice NAC transcription factor promotes leaf senescence via ABA biosynthesis. *Plant Physiol.* **174**: 1747–1763.
- Meng, F.W., Zhao, Q.Q., Zhao, X., Yang, C., Liu, R., Pang, J.H., Zhao, W.S., Wang, Q., Liu, M.X., Zhang, Z.G., et al. (2022). A rice protein modulates endoplasmic reticulum homeostasis and coordinates with a transcription factor to initiate blast disease resistance. *Cell Rep.* **39**: 110941.
- Meng, X.Q., Liu, S.Y., Dong, T.T., Xu, T., Ma, D.F., Pan, S.Y., Li, Z.Y., and Zhu, M.K. (2020). Comparative transcriptome and proteome analysis of salt-tolerant and salt-sensitive sweet potato and overexpression of *IbNAC7* confers salt tolerance in *Arabidopsis*. *Front. Plant Sci.* **11**: 572540.
- Meng, X.Q., Liu, S.Y., Zhang, C.B., He, J.N., Ma, D.F., Wang, X., Dong, T.T., Guo, F., Cai, J., Long, T.D., et al. (2023). The unique sweet potato NAC transcription factor *IbNAC3* modulates combined salt and drought stresses. *Plant Physiol.* **191**: 747–771.
- Michel, E., Salamini, R., Barelis, E., Dale, P., Baga, M., and Szalay, A. (1993). Analysis of a desiccation and ABA-responsive promoter isolated from the resurrection plant *Craterostigma plantagineum*. *Plant J.* **4**: 29–40.
- Michiels, C., Raes, M., Toussaint, O., and Remacle, J. (1994). Importance of Se-glutathione peroxidase, catalase, and Cu/Zn-SOD for cell survival against oxidative stress. *Free Radic. Biol. Med.* **17**: 235–248.
- Ming, R.H., Zhang, Y., Wang, Y., Khan, M., Dahro, B., and Liu, J.H. (2021). The JA-responsive MYC2-BADH-like transcriptional regulatory module in *Poncirus trifoliata* contributes to cold tolerance by modulation of glycine betaine biosynthesis. *New Phytol.* **229**: 2730–2750.
- Morreale, F.E., and Waldenand, H. (2016). Snapshot: Types of ubiquitin ligases. *Cell* **165**: 248.
- Munemasa, S., Oda, K., Watanabe-Sugimoto, M., Nakamura, Y., Shimoishi, Y., and Murata, Y. (2007). The coronatine-insensitive 1 mutation reveals the hormonal signaling interaction between abscisic acid and methyl jasmonate in *Arabidopsis* guard cells. Specific impairment of ion channel activation and second messenger production. *Plant Physiol.* **143**: 1398–1407.
- Nakashima, K., Takasaki, H., Mizoi, J., Shinozaki, K., and Yamaguchi-Shinozaki, K. (2012). NAC transcription factors in plant abiotic stress responses. *Biochim. Biophys. Acta* **1819**: 97–103.
- Olsen, A.N., Ernst, H.A., Leggio, L.L., and Skriver, K. (2005). NAC transcription factors: Structurally distinct, functionally diverse. *Trends. Plant. Sci.* **10**: 79–87.
- Pospilová, J. (2003). Participation of phytohormones in the stomatal regulation of gas exchange during water stress. *Biol. Plant.* **46**: 491–506.
- Puranik, S., Sahu, P.P., Srivastava, P.S., and Prasad, M. (2012). NAC proteins: Regulation and role in stress tolerance. *Trends. Plant. Sci.* **17**: 369–381.
- Qiu, Z.B., Guo, J.L., Zhu, A.J., Zhang, L., and Zhang, M.M. (2014). Exogenous jasmonic acid can enhance tolerance of wheat seedlings to salt stress. *Ecotoxicol. Environ. Saf.* **104**: 202–208.
- Raghavendra, A., and Reddy, K.B. (1987). Action of proline on stomata differs from that of abscisic acid, G-substances, or methyl jasmonate. *Plant Physiol.* **83**: 732–734.
- Rohwer, C.L., and Erwin, J.E. (2008). Horticultural applications of jasmonates. *J. Hortic. Sci. Biotech.* **83**: 283–304.
- Rouster, J., Leah, R., Mundy, J., and Cameron-Mills, V. (1997). Identification of a methyl jasmonate-responsive region in the promoter of a lipoxygenase 1 gene expressed in barley grain. *Plant J.* **11**: 513–523.
- Schmidt, S.B., Brown, L.K., Booth, A., Wishart, J., Hedley, P.E., Martin, P., Husted, S., George, T.S., and Russell, J. (2023). Heritage genetics for adaptation to marginal soils in barley. *Trends Plant Sci.* **28**: 544–551.
- Schmittgen, T.D., and Livak, K.J. (2008). Analyzing real-time PCR data by the comparative C(T) method. *Nat. Protoc.* **3**: 1101–1108.
- Seo, J.S., Joo, J.S., Kim, M.J., Kim, Y.K., Nahm, B.H., Song, S.I., Cheong, J.J., Lee, J.S., Kim, J.K., and Choi, Y.D. (2011). OsBHLH148, a basic helix-loop-helix protein, interacts with OsJAZ proteins in a jasmonate signaling pathway leading to drought tolerance in rice. *Plant J.* **65**: 907–921.
- Shang, X.G., Yu, Y.J., Zhu, L.J., Liu, H.Q., Chai, Q.C., and Guo, W.Z. (2020). A cotton NAC transcription factor GhirNAC2 plays positive roles in drought tolerance via regulating ABA biosynthesis. *Plant Sci.* **296**: 110498.
- Shinozaki, K., and Yamaguchi-Shinozaki, K. (2007). Gene networks involved in drought stress response and tolerance. *J. Exp. Bot.* **58**: 221–227.
- Simpson, S.D., Nakashima, K., Narusaka, Y., Seki, M., Shinozaki, K., and Yamaguchi-Shinozaki, K. (2003). Two different novel cis-acting elements of *ERD1*, a clpa homologous *Arabidopsis* gene function in induction by dehydration stress and dark-induced senescence. *Plant J.* **33**: 259–270.
- Singh, A.P., Mani, B., and Giri, J. (2021). OsJAZ9 is involved in water-deficit stress tolerance by regulating leaf width and stomatal density in rice. *Plant Physiol. Biochem.* **162**: 161–170.
- Squires, V.R., and Glenn, E.P. (2004). Salination, desertification, and soil erosion. In *The Role of Food, Agriculture, Forestry and Fisheries in Human Nutrition*. (Oxford, UK: UNESCO, EOLSS Publishers), pp, 102–123.

- Stone, S.L.** (2014). The role of ubiquitin and the 26S proteasome in plant abiotic stress signaling. *Front. Plant Sci.* **5**: 135.
- Su, Y.N., Huang, Y.Z., Dong, X.T., Wang, R.J., Tang, M.Y., Cai, J.B., Chen, J.Y., Zhang, X.Q., and Nie, G.** (2021). Exogenous methyl jasmonate improves heat tolerance of perennial ryegrass through alteration of osmotic adjustment, antioxidant defense, and expression of jasmonic acid-responsive genes. *Front. Plant Sci.* **12**: 664519.
- Tong, S.F., Chen, N.N., Wang, D.Y., Ai, F.D., Liu, B., Ren, L.W., Chen, Y., Zhang, J.L., Lou, S.L., Liu, H.H., et al.** (2021). The U-box E3 ubiquitin ligase PalPUB79 positively regulates ABA-dependent drought tolerance via ubiquitination of PalWRKY77 in populus. *Plant Biotechnol. J.* **19**: 2561–2575.
- Tran, L.S.P., Nakashima, K., Sakuma, Y., Simpson, S.D., Fujita, Y., Maruyama, K., Fujita, M., Seki, M., Shinozaki, K., and Yamaguchi-Shinozaki, K.** (2004). Isolation and functional analysis of *Arabidopsis* stress-inducible NAC transcription factors that bind to a drought responsive *cis*-element in the EARLY RESPONSIVE TO DEHYDRATION STRESS 1 promoter. *Plant Cell* **16**: 2481–2498.
- Trujillo, M., and Shirasu, K.** (2010). Ubiquitination in plant immunity. *Curr. Opin. Plant Biol.* **13**: 402–408.
- Umezawa, T., Fujita, M., Fujita, Y., Yamaguchi-Shinozaki, K., and Shinozaki, K.** (2006). Engineering drought tolerance in plants: Discovering and tailoring genes to unlock the future. *Curr. Opin. Biotechnol.* **17**: 113–122.
- Vierstra, R.D.** (2009). The ubiquitin-26s proteasome system at the nexus of plant biology. *Nat. Rev. Mol. Cell Biol.* **10**: 385–397.
- Walter, M., Chaban, C., Schütze, K., Batistic, O., Weckermann, K., Näke, C., Blazevic, D., Grefen, C., Schumacher, K., Oecking, C., et al.** (2004). Visualization of protein interactions in living plant cells using bimolecular fluorescence complementation. *Plant J.* **40**: 428–438.
- Wang, B., Zhai, H., He, S.Z., Zhang, H., Ren, Z.T., Zhang, D.D., and Liu, Q.C.** (2016). A vacuolar Na<sup>+</sup>/H<sup>+</sup> antiporter gene, *IbNHX2*, enhances salt and drought tolerance in transgenic sweetpotato. *Sci. Hortic. Amsterdam* **201**: 153–166.
- Wang, D.R., Zhang, X.W., Xu, R.R., Wang, G.L., You, C.X., and An, J.P.** (2022). Apple U-box-type E3 ubiquitin ligase MdPUB23 reduces cold-stress tolerance by degrading the cold-stress regulatory protein MdICE1. *Hortic. Res.* **9**: uhac171.
- Wang, Q., Yuan, F., Pan, Q.F., Li, M.Y., Wang, G.F., Zhao, J.Y., and Tang, K.X.** (2010). Isolation and functional analysis of the *Catharanthus roseus* deacetylchondoline-4-O-acetyltransferase gene promoter. *Plant Cell Rep.* **29**: 185–192.
- Wang, Y.C., Xu, H.F., Liu, W.J., Wang, N., Qu, C.Z., Jiang, S.H., Fang, H.C., Zhang, Z.Y., and Chen, X.S.** (2019). Methyl jasmonate enhances apple cold tolerance through the JAZ-MYC2 pathway. *Plant Cell Tissue Organ Cult.* **136**: 75–84.
- Wasternack, C., and Song, S.** (2017). Jasmonates: Biosynthesis, metabolism, and signaling by proteins activating and repressing transcription. *J. Exp. Bot.* **68**: 1303–1321.
- Wu, H., Ye, H.Y., Yao, R.F., Zhang, T., and Xiong, L.Z.** (2015). OsJAZ9 acts as a transcriptional regulator in jasmonate signaling and modulates salt stress tolerance in rice. *Plant Sci.* **232**: 1–12.
- Xiang, Y., Bian, X.L., Wei, T.H., Yan, J.W., Sun, X.J., Han, T., Dong, B.C., Zhang, G.F., Li, J., and Zhang, A.Y.** (2021b). ZmMPK5 phosphorylates ZmNAC49 to enhance oxidative stress tolerance in maize. *New Phytol.* **232**: 2400–2417.
- Xiang, Y., Sun, X.J., Bian, X.L., Wei, T.H., Han, T., Yan, J.W., and Zhang, A.Y.** (2021a). The transcription factor ZmNAC49 reduces stomatal density and improves drought tolerance in maize. *J. Exp. Bot.* **72**: 1399–1410.
- Xiao, L.Y., Shi, Y.Y., Wang, R., Feng, Y., Wang, L.S., Zhang, H.S., Shi, X.Y., Jing, G.Q., Deng, P., Song, T.Z., et al.** (2022). The transcription factor OsMYBc and an E3 ligase regulate expression of a K<sup>+</sup> transporter during salt stress. *Plant Physiol.* **190**: 843–859.
- Xing, Q.J., Liao, J.J., Cao, S.X., Li, M., Lv, T.H., and Qi, H.Y.** (2020). CmLOX10 positively regulates drought tolerance through jasmonic acid-mediated stomatal closure in oriental melon (*Cucumis melo* var. *makuwa* Makino). *Sci. Rep.* **10**: 17452–17465.
- Xu, B.Q., Wang, J.J., Peng, Y., Huang, H., Sun, L.L., Yang, R., Suo, L.N., Wang, S.H., and Zhao, W.C.** (2022). SIMYC2 mediates stomatal movement in response to drought stress by repressing *SICHS1* expression. *Front. Plant Sci.* **13**: 952758.
- Xu Z.Y., Gongbuzhaxi, Wang C.Y., Xue F., Zhang H., Ji W.Q.** (2015) Wheat NAC transcription factor *TaNAC29* is involved in response to salt stress. *Plant Physiol. Biochem.* **96**: 356–363.
- Yamaguchi, M., Ohtani, M., Mitsuda, N., Kubo, M., Ohme-Takagi, M., Fukuda, H., and Demura, D.** (2010). VND-INTERACTING2, a NAC domain transcription factor, negatively regulates xylem vessel formation in *Arabidopsis*. *Plant Cell* **22**: 1249–1263.
- Yamasato, A., Nagata, N., Tanaka, R., and Tanaka, A.** (2005). The N-terminal domain of chlorophyllide an oxygenase confers protein instability in response to chlorophyll b accumulation in *Arabidopsis*. *Plant Cell* **17**: 1585–1597.
- Yan, Z., Zhang, W., Chen, J., and Li, X.** (2015). Methyl jasmonate alleviates cadmium toxicity in *Solanum nigrum* by regulating metal uptake and antioxidative capacity. *Biol. Plant.* **59**: 373–381.
- Yang, Y.F., Wang, Y.N., Jia, L.C., Yang, G.H., Xu, X.Z., Zhai, H., He, S.Z., Li, J.X., Dai, X.D., Qin, N., et al.** (2018). Involvement of an ABI-like protein and a Ca<sup>2+</sup>-ATPase in drought tolerance as revealed by transcript profiling of a sweetpotato somatic hybrid and its parents *Ipomoea batatas* (L.) Lam. and *I. triloba* L. *PLoS ONE* **13**: e0193193.
- You, J., Zong, W., Li, X.K., Ning, J., Hu, H.H., Li, X.H., Xiao, J.H., and Xiong, L.Z.** (2013). The SNAC1-targeted gene *OsSRO1c* modulates stomatal closure and oxidative stress tolerance by regulating hydrogen peroxide in rice. *J. Exp. Bot.* **64**: 569–583.
- Yu, F.F., Wu, Y.R., and Xie, Q.** (2016). Ubiquitin-proteasome system in aba signaling: From perception to action. *Mol. Plant* **9**: 21–33.
- Yu, Y.C., Xu, T., Li, X., Tang, J., Ma, D.F., Li, Z.Y., and Sun, J.** (2016). NaCl-induced changes of ion homeostasis and nitrogen metabolism in two sweet potato (*Ipomoea batatas* L.) cultivars exhibit different salt tolerance at adventitious root stage. *Environ. Exp. Bot.* **129**: 23–36.
- Zhai, H., Wang, F.B., Si, Z.Z., Huo, J.X., Xing, L., An, Y.Y., He, S.Z., and Liu, Q.C.** (2016). A myo-inositol-1-phosphate synthase gene, *IbMIPS1*, enhances salt and drought tolerance and stem nematode resistance in transgenic sweet potato. *Plant Biotechnol. J.* **14**: 592–602.
- Zhang, H., Gao, X.R., Zhi, Y.H., Li, X., Zhang, Q., Niu, J.B., Wang, J., Zhai, H., Zhao, N., Li, J.G., et al.** (2019). A non-tandem CCCH-type zinc-finger protein, IbC3H18, functions as a nuclear transcriptional activator and enhances abiotic stress tolerance in sweet potato. *New Phytol.* **223**: 1918–1936.
- Zhang, H., Wang, Z., Li, X., Gao, X.R., Dai, Z.R., Cui, Y.F., Zhi, Y.H., Liu, Q.C., Zhai, H., Gao, S.P., et al.** (2022). The IbBBX24-IbTOE3-IbPRX17 module enhances abiotic stress tolerance by scavenging reactive oxygen species in sweet potato. *New Phytol.* **233**: 1133–1152.
- Zhang, H., Zhang, Q., Wang, Y.N., Li, Y., Zhai, H., Liu, Q.C., and He, S.Z.** (2017a). Characterization of salt tolerance and fusarium wilt tolerance of a sweetpotato mutant. *J. Integr. Agr.* **16**: 1946–1955.
- Zhang, H., Zhang, Q., Zhai, H., Li, Y., Wang, X.F., Liu, Q.C., and He, S.Z.** (2017b). Transcript profile analysis reveals important roles of jasmonic acid signalling pathway in the response of sweet potato to salt stress. *Sci. Rep.* **7**: 40819.
- Zheng, X.N., Chen, B., Lu, G.J., and Han, B.** (2009). Overexpression of a NAC transcription factor enhances rice drought and salt tolerance. *Biochem. Biophys. Res. Commun.* **379**: 985–989.
- Zheng, X.Y., Spivey, N.W., Zeng, W., Liu, P.P., Fu, Z.Q., Klessig, D.F., He, S.Y., and Dong, X.** (2012). Coronatine promotes *Pseudomonas syringae* virulence in plants by activating a signaling cascade that inhibits salicylic acid accumulation. *Cell Host Microbe* **11**: 587–596.

## IbNAC087 regulates abiotic stress response

Zhou, Y., Li, X.H., Guo, Q.H., Liu, P., Li, Y., Wu, C.A., Yang, G.D., Huang, J.G., Zhang, S.Z., Zheng, C.C., et al. (2021). Salt responsive alternative splicing of a RING finger E3 ligase modulates the salt stress tolerance by fine-tuning the balance of COP9 signalosome subunit 5A. *PLoS Genet.* **17**: e1009898.

Zhu, J.T., Wei, X.N., Yin, C.S., Zhou, H., Yan, J.H., He, W.X., Yan, J.B., and Li, H. (2023). ZmEREB57 regulates OPDA synthesis and enhances salt stress tolerance through two distinct signaling pathways in *Zea mays*. *Plant Cell Environ.* **46**: 2867–2883.

## SUPPORTING INFORMATION

Additional Supporting Information may be found online in the supporting information tab for this article: <http://onlinelibrary.wiley.com/doi/10.1111/jipb.13612/supinfo>

**Figure S1.** Phylogenetic tree of IbNAC087 and NAC (NAM, ATAF1/2, and CUC2) DOMAIN CONTAINING PROTEINs (ANACs) in *Arabidopsis*

**Figure S2.** Phylogenetic analysis of IbNAC087 and its homologs in different plant species

**Figure S3.** Multiple sequence alignment of IbNAC087 and its homologs in different plant species

**Figure S4.** Diagrammatic representation of the *IbNAC087* promoter showing the positions of various *cis*-acting elements

**Figure S5.** Production of *IbNAC087* transgenic sweet potato plants

**Figure S6.** Responses of *IbNAC087*-OE (overexpression) and wild-type (WT) sweet potato plants cultured for 4 weeks on Murashige and Skoog medium without stress, with 200 mmol/L NaCl or 20% polyethylene glycol (PEG)6000, respectively

**Figure S7.** Responses of *IbNAC087*-transgenic lines and wild-type (WT) grown in transplanting boxes without stress or with 200 mmol/L NaCl and drought stresses

**Figure S8.** Time-course phenotypes of *IbNAC087*-transgenic and wild-type (WT) plants grown in transplanting boxes under stresses

**Figure S9.** Overexpression of *IbNAC087* in sweet potato up-regulates abiotic stress-responsive genes under salt and drought stresses

**Figure S10.** Exogenous methyl jasmonate (MeJA) application effectively promoted stomatal closure and enhanced reactive oxygen species (ROS) scavenging in *IbNAC087*-OE (overexpression) plants

**Figure S11.** The purification of the recombinant His-IbNAC087 protein

**Figure S12.** Overexpressing of *IbLOX* and *IbAOS* enhanced salt and drought tolerance in sweet potato

**Figure S13.** Sequence and expression analysis of *IbNIEL*

**Figure S14.** The purification of the recombinant glutathione S-transferase – NAC087-INTERACTING E3 LIGASE (GST-IbNIEL) protein

**Figure S15.** Production of overexpression *IbNIEL* transgenic sweet potato plants

**Figure S16.** Responses, main root length, and fresh weight (FW) of *IbNIEL*-OE (overexpression) and wild-type (WT) sweet potato plants cultured for 4 weeks on Murashige and Skoog medium without stress, with 86 mmol/L NaCl or 20% polyethylene glycol (PEG)6000, respectively.

**Figure S17.** Jasmonic acid (JA) content, superoxide dismutase (SOD) and peroxidase (POD) activities, malondialdehyde (MDA) and H<sub>2</sub>O<sub>2</sub> contents of *IbNIEL* transgenic plants in transplanting boxes and incubated without stress or with 200 mmol/L NaCl for 2 weeks or drought treatment (without water) for 3 weeks

**Figure S18.** Time-course phenotypes of *IbNIEL*-OE (overexpression) and wild-type (WT) plants grown in transplanting boxes under stresses

**Figure S19.** Observation of stomata of field-grown *IbNIEL*-OE (overexpression) and wild-type (WT) plants under normal conditions or treated with 200 mmol/L NaCl, 20% polyethylene glycol (PEG), or 20 μmol/L methyl jasmonate (MeJA)

**Figure S20.** Overexpression of *IbNIEL* in sweet potato down-regulates abiotic stress-responsive genes under salt and drought stresses

**Table S1.** The expression patterns of the candidate abiotic-related transcription factors (TFs) as determined by RNA sequencing

**Table S2.** The amino acid species statistics of *IbNAC087*<sup>C84</sup>

**Table S3.** Comparison of *IbNAC087*-OE (overexpression) transgenic plants with wild-type (WT) after 4 weeks of culture on Murashige and Skoog medium with or without 200 mmol/L NaCl and 20% polyethylene glycol (PEG)

**Table S4.** Comparison of *IbNAC087* transgenic plants with wild-type (WT) plants under salt and drought treatments

**Table S5.** Comparison of *IbNAC087* transgenic plants with wild-type (WT) plants under salt and drought stresses with or without methyl jasmonate (MeJA) treatment

**Table S6.** The NAC-binding motifs in the 2,000 bp promoter regions of jasmonic acid (JA) biosynthesis-related genes

**Table S7.** Comparison of *IbLOX* and *IbAOS* transgenic plants with wild-type (WT) plants under salt and drought treatments

**Table S8.** List of *IbNAC087*-interacting proteins, as identified by yeast two-hybrid (Y2H) assays

**Table S9.** Comparison of *IbNIEL*-OE (overexpression) transgenic plants with wild-type (WT) after 4 weeks of culture on Murashige and Skoog medium with or without 200 mmol/L NaCl and 20% polyethylene glycol (PEG)

**Table S10.** Comparison of *IbNIEL* transgenic plants with wild-type (WT) plants under NaCl treatment

**Table S11.** Comparison of *IbNIEL* transgenic plants with wild-type (WT) plants under drought treatment

**Table S12.** Sequences of the primers used in this study



Scan using WeChat with your smartphone to view JIPB online



Scan with iPhone or iPad to view JIPB online